

Th17 generation.^{7,8,14} The RA-dependent generation of gut-tropic Foxp3⁺ inducible regulatory T cells appears to be important for oral tolerance.^{15–17} However, the generation of Th1 and Th17 cells also appears to require RA.^{18,19} Furthermore, in conjunction with IL-15, RA acts as an adjuvant to promote Th1-dependent inflammation.²⁰ VA or RA deficiency also affects the nature of DCs, especially mesenteric lymph node (MLN)-DCs. RALDH2 expression is nearly absent in MLN-DCs of VA(–) mice.^{6,9,21} The langerin⁺ CD8 α [–] CD11b^{low}/⁺ CD103⁺ DC population increases in MLNs.²²

Here we unexpectedly found that MLN-DCs of unprimed VA(–) mice induced the differentiation of naive CD4⁺ T cells to a distinct subset of inflammatory Th2 cells that particularly produced high levels of interleukin-13 (IL-13) and tumor necrosis factor- α (TNF- α) as well as Th17 cells. IL-6- and OX40 ligand (OX40L)-mediated signals appeared to be required for the optimal induction of these IL-13-producing inflammatory Th2 cells, whereas TGF- β suppressed the induction. Th17 cytokines contribute to inflammatory and autoimmune diseases,²³ whereas IL-13 plays critical roles in inflammatory and allergic diseases including asthma,^{24–27} ulcerative colitis,^{28,29} and atopic dermatitis.³⁰ IL-13 is also a major stimulator of tissue remodeling and fibrosis in various tissues, including the liver, lungs, and skin.²⁵ Thus, we speculated that MLN-DCs of VA(–) mice (VA(–)MLN-DCs) may participate in the induction of oral antigen-specific inflammatory or allergic responses in an IL-13-dependent manner. Indeed, VA(–) mice that received repeated oral antigen administration exhibited IL-13-dependent strong IgG1 responses and subsequent IgE responses upon antigen challenge with an adjuvant. We suggest that RA plays a critical role in the inhibition of inflammatory or allergic responses to oral antigens partly by preventing MLN-DCs from inducing IL-13-producing inflammatory Th2 cells.

RESULTS

MLN-DCs of VA(–) mice efficiently induce IL-13-producing inflammatory Th2 cells and Th17 cells

We first evaluated the ability of DCs obtained from various lymphoid organs of VA(–) and VA(+) mice to induce functional naive CD4⁺ T-cell differentiation. VA(–)MLN-DCs induced T cells to express markedly higher levels of E- and P-selectin ligands, *Ccr2*, *Ccr4*, *Ccr5*, and *Ccr6*, but lower levels of *Ccr9* compared with VA(+)MLN-DCs (Figure 1a–c). The proteins encoded by these genes are involved in T-cell homing to inflammatory sites or the skin.³¹ Indeed, T cells activated with VA(–)MLN-DCs preferentially migrated into inflamed skin (Figure 1d). In the presence of TGF- β , VA(+)MLN-DCs induced the expression of Foxp3 and CD103 on T cells, whereas VA(–)MLN-DCs induced the weak expression of these molecules (Figure 1e). VA deficiency had a much lesser impact on the ability of DCs from other lymphoid organs to induce T cells to express these molecules, except for splenic (SPL)-DCs, and induce *Ccr4* expression (Figure 1a,b).

T cells induced by VA(–)MLN-DCs produced higher levels of IL-4, IL-9, IL-13, IL-17A, IL-21, and TNF- α upon activation

than those induced by VA(+)MLN-DCs (Figure 2a). In particular, IL-13 and TNF- α levels were strikingly higher. Most of the IL-13-producing T cells expressed TNF- α but not interferon- γ (IFN- γ) or IL-17A (Figure 2b), suggesting that these T cells were inflammatory Th2 cells. However, they produced low levels of IL-5 unlike previously described inflammatory Th2 cells (Figure 2a).³² Thus, these IL-13-producing T cells appear to be a distinct subset of inflammatory Th2 cells. On the other hand, T cells induced by DCs from Peyer's patches (PPs) of VA(–) or VA(+) mice produced low levels of cytokines except for IFN- γ (Figure 2a). T cells induced by DCs from the skin-draining peripheral lymph nodes (PLNs) of VA(–) mice produced significantly higher levels of IL-17A, IL-21, and TNF- α , and lower levels of IFN- γ , IL-4, and IL-10 than those induced by VA(+)PLN-DCs. T cells induced by VA(–)SPL-DCs produced higher levels of IFN- γ and IL-10 than those induced by VA(+)SPL-DCs, but their production levels of other cytokines were low. These results suggest that VA deficiency facilitates PLN-DCs to induce Th17 cells, but most strikingly affects the nature of MLN-DCs and causes them to induce IL-13-producing inflammatory Th2 and Th17 cells that express homing receptors for inflammatory sites or the skin.

VA deficiency enhances inflammatory signatures in conventional DCs (cDCs) of MLNs

VA(–)MLN-DCs expressed higher levels of *Il6*, *Il12b* (encodes IL-12p40), and *Tnfsf4* (encodes OX40L), but lower levels of *Il10*, *Tgfb1*, and *Mmp9* (encoding matrix metalloproteinase 9 that activates TGF- β) compared with VA(+)MLN-DCs (Figure 3a). Thus, VA(–)MLN-DCs may have a predominant inflammatory nature.

B220[–] cDCs from VA(–)MLNs expressed higher levels of CD40, CD86, and major histocompatibility complex class II, but lower levels of CD103 than those from VA(+)MLNs (Figure 3b). On the other hand, VA deficiency did not significantly affect the surface marker expression on PP-cDCs or B220⁺ plasmacytoid DCs (pDCs) of MLNs (Supplementary Figure S1 online). In PP-pDCs, however, VA deficiency increased the proportion of CCR9⁺ CD8 α ⁺ CD40[–] CD80[–] CD86[–] major histocompatibility complex class II^{low} cells (Supplementary Figure S1b), the phenotype of which resembled that of tolerogenic CCR9⁺ pDCs.³³ The VA status did not significantly affect surface marker expression on SPL-DCs and PLN-DCs (data not shown). These results collectively suggest that VA deficiency increases the proportion of inflammatory mature or activated cells in the MLN-cDC population.

The CD8 α [–] CD11b⁺ CD103[–] cDC subset of MLNs in VA(–) mice instructs naive CD4⁺ T cells to differentiate into IL-13-producing inflammatory Th2 cells in an IL-6-dependent manner

To identify the DC subset responsible for IL-13-producing inflammatory Th2 induction, we fractionated VA(–)MLN-DCs (Figure 3c). VA deficiency most strikingly affected surface marker expression in the CD8 α [–] CD11b⁺ CD103[–] cDC (R2)

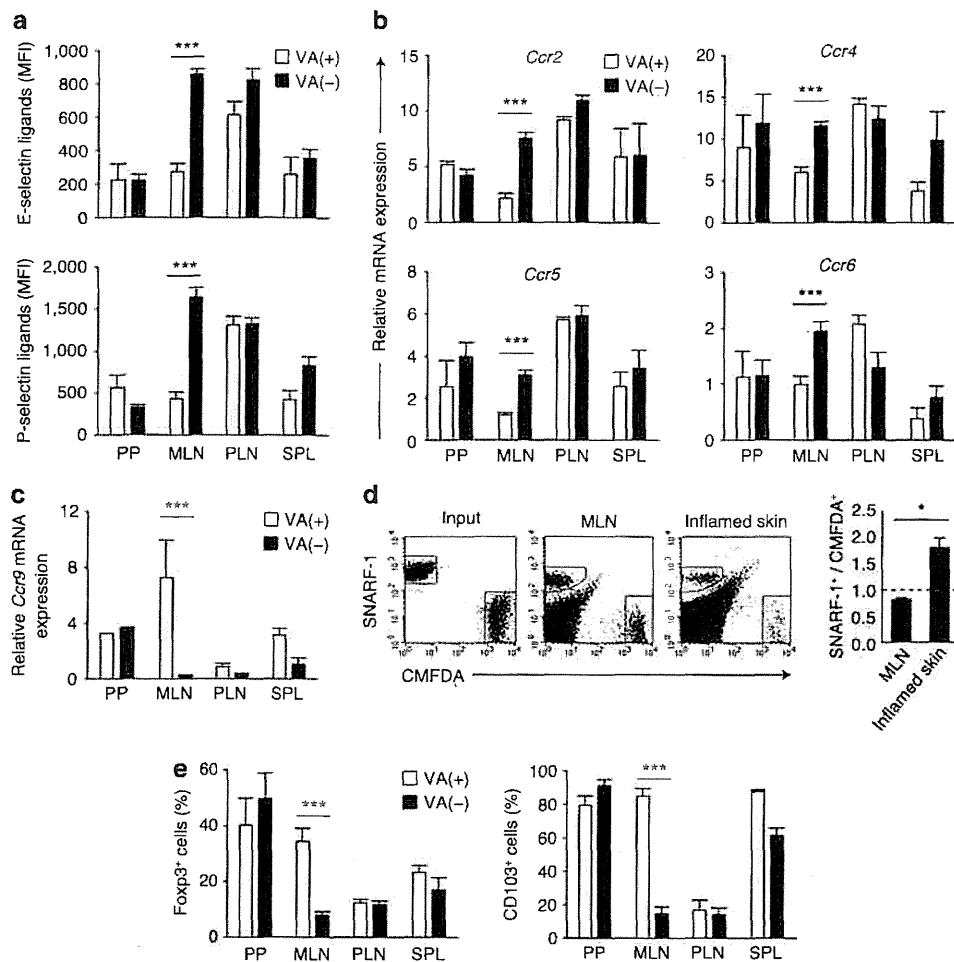


Figure 1 Dendritic cells (DCs) from mesenteric lymph nodes (MLNs) of vitamin A-deficient (VA(-)) mice instruct T cells to express homing receptors for inflammatory sites or skin. (a) CD4⁺ T cells from DO11.10/*Rag2*^{-/-} mice were stimulated with ovalbumin (OVA) peptide and DCs from Peyer's patches (PPs), MLNs, peripheral lymph nodes (PLNs), or spleens (SPLs) of VA(+) or VA(-) mice. Expression of E- and P-selectin ligands on the T cells was analyzed by flow cytometry. Data are expressed as mean fluorescence intensities (MFIs). (b) mRNA expression of chemokine receptors in CD4⁺ T cells stimulated as above was analyzed by real-time PCR. Levels of relative mRNA expression are shown. (c) CD4⁺ T cells were stimulated with OVA peptide-pulsed DCs from the indicated tissue of VA(+) or VA(-) mice. Relative *Ccr9* mRNA expression in the T cells is shown. (d) CD4⁺ T cells were stimulated with MLN-DCs from VA(+) or VA(-) mice as in a, and were differentially labeled with 5-chloromethyl/fluorescein diacetate (CMFDA) and SNARF[®]-1 carboxylic acid acetate succinimidyl ester (SNARF-1). Equal cell numbers of each preparation were mixed and injected intravenously into recipient mice with preexisting cutaneous inflammation in ears induced by 2,4-dinitro-1-fluorobenzene-induced delayed hypersensitivity. After 16 h, the transferred cells were recovered from recipient tissues and analyzed by flow cytometry. Representative flow cytometry dot plots are shown. The ratios of SNARF-1⁺ cells/CMFDA⁺ cells from MLNs and both ears (inflamed skin) are shown as mean \pm s.e.m., $n = 4$ recipient mice. * $P < 0.05$. (e) Flow cytometric analysis of forkhead box P3 (Foxp3) and CD103 expression in CD4⁺ T cells stimulated with OVA peptide and the indicated DCs in the presence of transforming growth factor- β . Data are presented as mean \pm s.d. of quadruplicate samples. Representative results from three independent experiments are shown. *** $P < 0.001$.

subset (Figure 3d). The R2 subset expressed *Il6*, *Il12b*, and *Tnfsf4*, but only low levels of *Il12a* (encodes IL-12p35) and *Il23a* (encodes IL-23p19) (Figure 3e). VA deficiency especially enhanced the expression of *Il6*, *Il12b*, and *Tnfsf4*. IL-13-producing cells were induced most strongly by R2, moderately by the CD8 α ⁻CD11b⁺CD103⁺ cDC (R3) subset, and weakly by the other cDC subsets (Figure 4a). However, IL-17A-producing cells were induced most strongly by R3 and slightly less strongly by R2. Both R2 and R3 induced TNF- α -producing cells. IFN- γ -producing cells were most efficiently induced by the CD8 α ⁺CD11b⁻ cDC (R1) subset and less efficiently by R2 (Figure 4a). T cells stimulated with R2 or R3 expressed *Ccr2*, *Ccr4*, *Ccr5*, and *Ccr6* (Supplementary Figure S2a)

and high levels of E- and P-selectin ligands (Supplementary Figure S2b). The results suggest that R2 and R3 most efficiently induce IL-13-producing inflammatory Th2 and Th17, respectively, and that these T cells are tropic to the skin or inflammatory sites.

We then analyzed the mechanism of IL-13-producing inflammatory Th2 induction by R2. An IL-6-neutralizing antibody inhibited the induction of IL-13-, IL-17A-, or TNF- α -producing T cells (Figure 4b). Neutralizing antibodies against IL-12p40 and IL-23p19 suppressed the induction of IL-13-producing cells but not of IL-17A-producing cells. The results suggest that IL-6 and monomeric IL-12p40 or its homodimer IL-12p80 participate in IL-13-producing inflammatory Th2

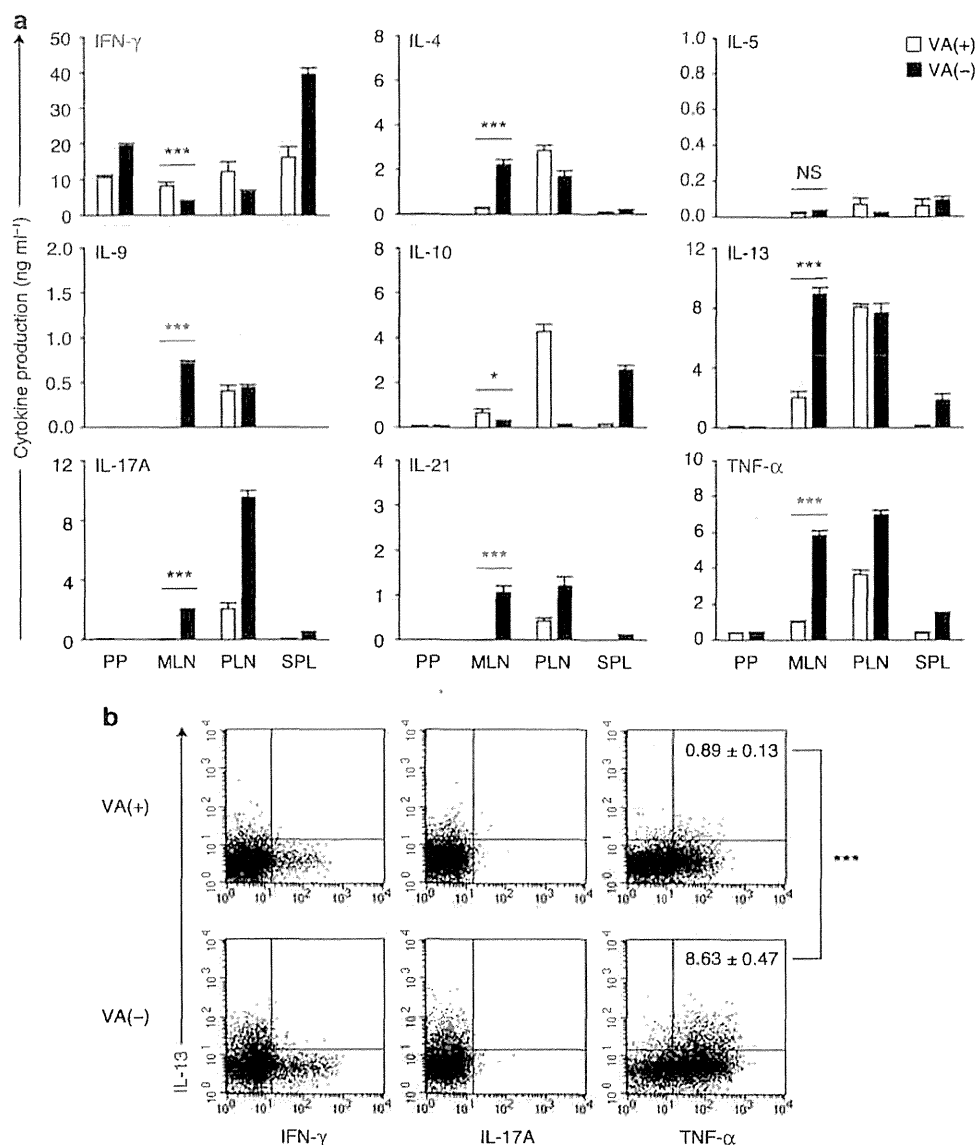


Figure 2 Dendritic cells (DCs) from mesenteric lymph nodes (MLNs) of vitamin A-deficient (VA(-)) mice instruct T cells to differentiate into interleukin-13 (IL-13)-producing inflammatory T helper type 2 (Th2) cells. (a) CD4⁺ T cells from DO11.10/*Rag2*^{-/-} mice were stimulated with ovalbumin (OVA) peptide and DCs from Peyer's patches (PPs), MLNs, peripheral lymph nodes (PLNs), or spleens (SPLs) of VA(+) or VA(-) mice, and were restimulated with immobilized monoclonal antibodies to CD3 and CD28. Cytokine concentrations in the supernatants were assessed by enzyme-linked immunosorbent assay. Data are presented as mean \pm s.d. of quadruplicate samples. * P < 0.05; *** P < 0.001; NS, not significant. Representative results from three independent experiments are shown. IFN- γ , interferon- γ . (b) CD4⁺ T cells were stimulated with OVA peptide and MLN-DCs from VA(+) or VA(-) mice, and were restimulated with immobilized anti-CD3 and soluble anti-CD28 in the presence of monensin. Representative flow cytometry dot plots (from three independent experiments) of intracellular cytokine expression are shown. The percentage of IL-13⁺ tumor necrosis factor (TNF)- α ⁺ cells is shown as mean \pm s.d. of quadruplicate samples. *** P < 0.001.

induction and that IL-6 but not IL-12p40 is required for Th17 induction. The balance between the IL-13-producing inflammatory Th2 and Th17 subsets in T cells stimulated with VA(-)MLN-cDCs slightly varied according to the experiments. OX40L expression on DCs is known to contribute to the induction of inflammatory Th2 cells.³² An OX40L-blocking antibody partly inhibited the ability of R2 to induce IL-13-producing T cells, but enhanced its ability to induce IL-17A-producing T cells (Figure 4b). These results suggest that IL-6 is essential for the induction of

both IL-13-producing inflammatory Th2 and Th17 cells, and that OX40L-mediated signals affect the IL-13-producing inflammatory Th2/Th17 balance.

RA receptor (RAR)-mediated signals prevent MLN-DCs from inducing IL-13-producing inflammatory Th2 differentiation

RAR-mediated signals can contribute to DC homeostasis in an autocrine or paracrine manner in the MLNs of normal and VA(+) mice. Indeed, RA prevented VA(-)MLN-DCs from

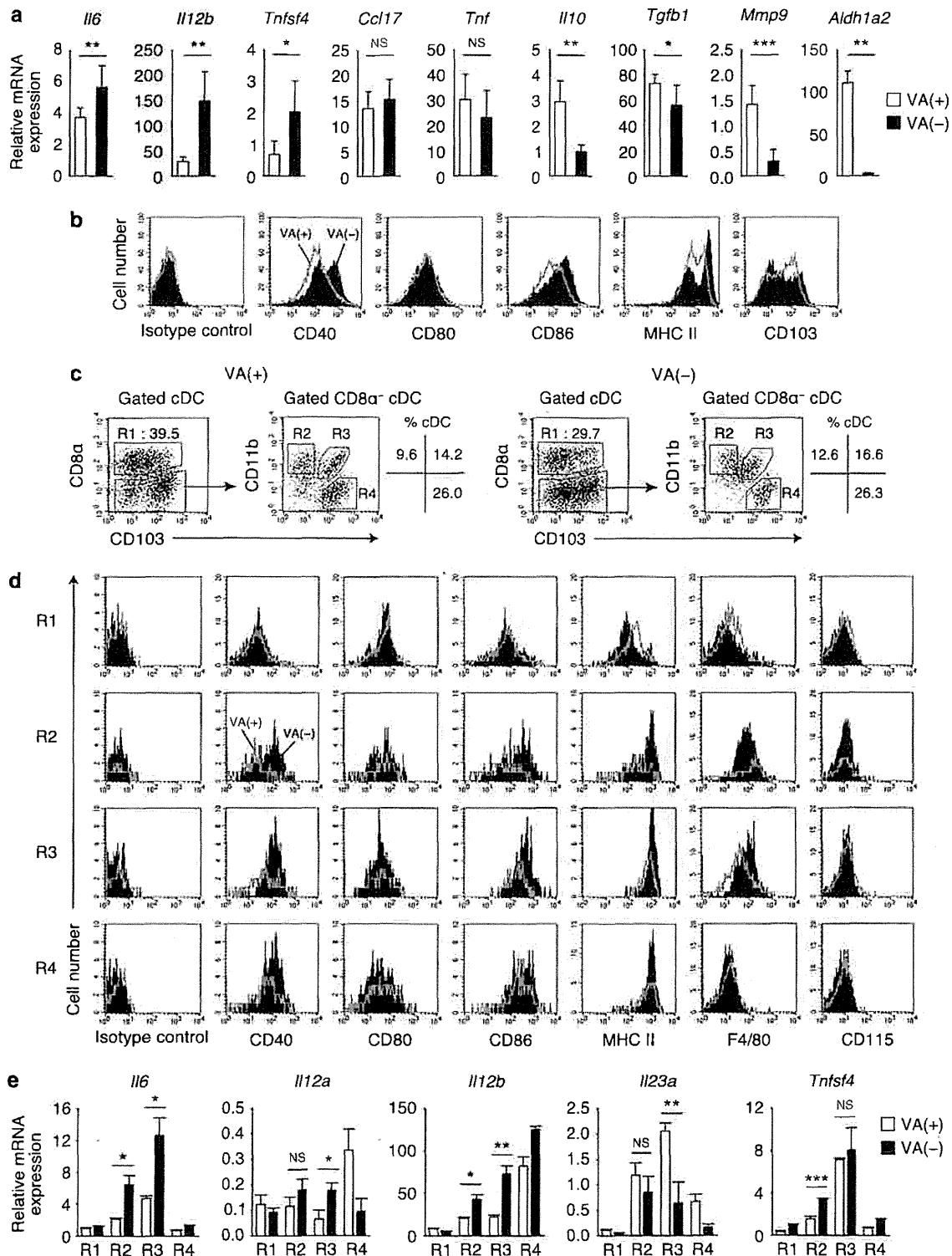


Figure 3 The $CD8\alpha^- CD11b^+ CD103^-$ subset of conventional dendritic cells (cDCs) from mesenteric lymph nodes (MLNs) of vitamin A-deficient ($VA(-)$) mice exhibits more inflammatory phenotypes than $VA(+)$ MLN-DCs. **(a)** Relative mRNA expression of indicated genes in total $CD11c^+$ cells from MLNs of $VA(+)$ and $VA(-)$ mice. Data are presented as mean \pm s.d. of triplicate samples. Representative results from three independent experiments are shown. * $P < 0.05$; ** $P < 0.01$; *** $P < 0.001$; NS, not significant. **(b)** Representative flow cytometry histograms (from three independent experiments) of the expression of the indicated molecules on gated $B220^- CD11c^+$ cDCs from MLNs of $VA(+)$ (solid line) and $VA(-)$ mice (shaded histogram). **(c)** Scheme for sorting MLN-DC subsets from $VA(+)$ and $VA(-)$ mice. Left dot plots show division of $B220^- CD11c^+$ cDCs into two major $CD8\alpha^+$ (R1) and $CD8\alpha^-$ subsets. $CD8\alpha^-$ cDCs were further subdivided into $CD11b^+ CD103^-$ (R2), $CD11b^+ CD103^+$ (R3), and $CD11b^- CD103^+$ (R4) subsets. **(d)** Representative flow cytometry histograms (from three independent experiments) of the surface expression of the indicated molecules on MLN-DC subsets from $VA(+)$ (solid line) and $VA(-)$ mice (shaded histogram). **(e)** Relative mRNA expression of the indicated molecules in MLN-DC subsets from $VA(+)$ and $VA(-)$ mice. Data are presented as mean \pm s.d. of triplicate samples. Representative results from three independent experiments are shown.

inducing T cells that produced high levels of IL-13, IL-17A, TNF- α , or IFN- γ (Figure 5a). However, the RAR antagonists LE135 or LE540 enhanced the ability of MLN-DCs of normal mice to induce IL-13-, IL-17A-, or TNF- α -producing T cells (Figure 5b). In the presence of LE135 or LE540, the CD8 α ⁻CD11b⁺CD103⁻ (R2) MLN-cDC subset of normal mice induced T cells that produced high levels of IL-13, IL-17A, and TNF- α (Figure 5c). IL-17A-producing T cells were also induced by the CD8 α ⁻CD11b⁺CD103⁺ (R3) subset in the presence of LE540, but not by the CD8 α ⁺CD11b⁻CD103^{-/+}

(R1) and CD8 α ⁻CD11b⁻CD103⁺ (R4) subsets. R1 induced IFN- γ -producing T cells in the presence of LE135. Importantly, each cDC subset was differentially affected by RAR antagonists with regard to the induction of cytokine-producing T cells. The LE540-dependent normal R2-mediated induction of IL-13-, IL-17A-, and TNF- α -producing T-cell subsets was abrogated by a neutralizing antibody against IL-6 and partly abrogated by an antibody against IL-12p40 (Figure 5d). A blocking antibody against OX40L partly inhibited the induction of IL-13- and TNF- α -producing T cells but not of IL-17A-producing T cells.

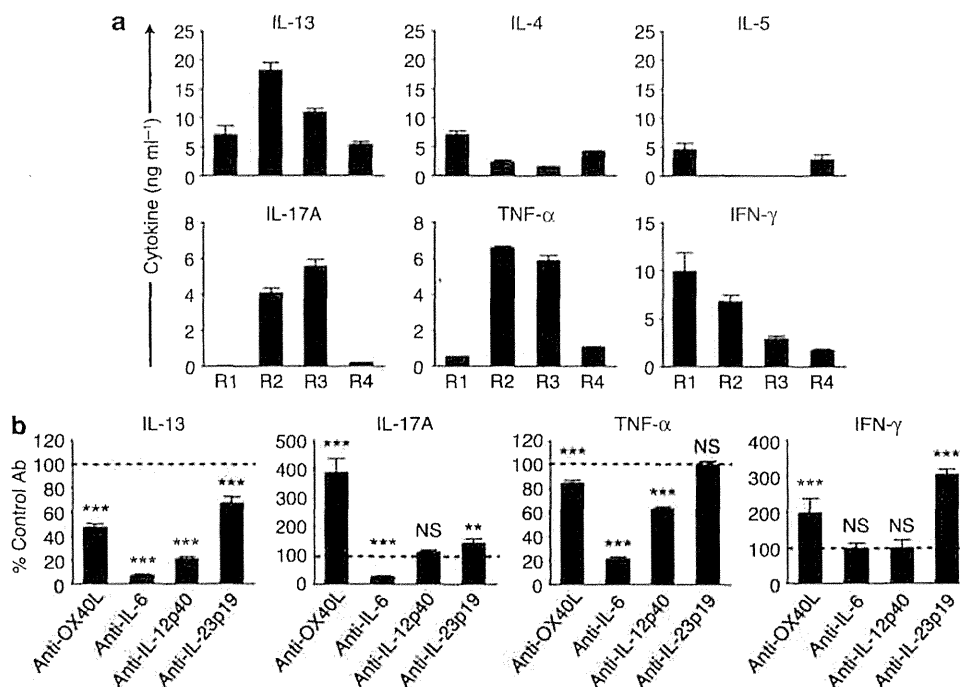


Figure 4 The CD8 α ⁻CD11b⁺CD103⁻ subset of conventional dendritic cells (cDCs) from mesenteric lymph nodes (MLNs) of vitamin A-deficient (VA(-)) mice most efficiently induces interleukin-13 (IL-13)-producing inflammatory T helper type 2 (Th2) differentiation. (a) CD4⁺ T cells from DO11.10/*Rag2*^{-/-} mice were stimulated with ovalbumin (OVA) peptide and MLN-DC subsets (R1, CD8 α ⁺CD11b⁻CD103^{+/-} cDCs; R2, CD8 α ⁻CD11b⁺CD103⁻ cDCs; R3, CD8 α ⁻CD11b⁺CD103⁺ cDCs; R4, CD8 α ⁻CD11b⁻CD103⁺ cDCs) from VA(-) mice, and were restimulated with immobilized monoclonal antibodies (mAbs) to CD3 and CD28. Cytokine concentrations in the supernatants were assessed by enzyme-linked immunosorbent assay (ELISA). (b) CD4⁺ T cells were stimulated with OVA peptide and CD8 α ⁻CD11b⁺CD103⁻ (R2) subset of MLN-cDCs from VA(-) mice in the presence of anti-OX40L, anti-IL-6, anti-IL-12p40, anti-IL-23p19, or isotype control mAbs, and were restimulated with immobilized mAbs to CD3 and CD28. Cytokine concentrations in the supernatants were assessed by ELISA. Results are shown as the percentage of the control culture with the isotype control mAb. Data are presented as mean \pm s.d. of quadruplicate. ***P* < 0.01; ****P* < 0.001; NS, not significant vs. control mAb. Representative results from three independent experiments are shown.

Figure 5 Retinoic acid receptor (RAR)-mediated signals prevent dendritic cells (DCs) of mesenteric lymph nodes (MLNs) from inducing interleukin-13 (IL-13)-producing inflammatory T helper type 2 (Th2) differentiation. (a) CD4⁺ T cells from DO11.10/*Rag2*^{-/-} mice were stimulated with ovalbumin (OVA) peptide and MLN-DCs from vitamin A-deficient (VA(-)) or VA(+) mice in the presence or absence of RA, and restimulated with immobilized monoclonal antibodies (mAbs) to CD3 and CD28. Cytokine concentrations in the supernatants were assessed by enzyme-linked immunosorbent assay (ELISA). **P* < 0.05; ***P* < 0.01; ****P* < 0.001; NS, not significant. (b) CD4⁺ T cells were stimulated with OVA peptide and (b) whole MLN-DCs or (c) MLN-DC subsets (R1, CD8 α ⁺CD11b⁻CD103^{+/-} cDCs; R2, CD8 α ⁻CD11b⁺CD103⁻ cDCs; R3, CD8 α ⁻CD11b⁺CD103⁺ cDCs; R4, CD8 α ⁻CD11b⁻CD103⁺ cDCs) of normal mice in the presence or absence of LE135 or LE540, and were restimulated with immobilized mAbs to CD3 and CD28. Cytokine concentrations in the supernatants were assessed by ELISA. **P* < 0.05; ***P* < 0.01; ****P* < 0.001 vs. absence of LE135 and LE540. (d) CD4⁺ T cells were stimulated with OVA peptide, LE540, and the CD8 α ⁻CD11b⁺CD103⁻ (R2) subset of MLN-cDCs from normal mice in the presence of anti-OX40L, anti-IL-6, anti-IL-12p40, or isotype control mAbs, and were restimulated with immobilized mAbs to CD3 and CD28. Cytokine concentrations in the supernatants were assessed by ELISA. Results are shown as the percentage of the control culture with the isotype control mAb. **P* < 0.05; ***P* < 0.01; ****P* < 0.001; NS, not significant vs. control mAb. Data are presented as mean \pm s.d. of quadruplicate samples. Representative results from three independent experiments are shown.

These results suggest that in normal mice, MLN-DCs possess the latent ability to induce IL-13-producing inflammatory Th2 and Th17 cell differentiation, and that RA prevents the differentiation of these T cells by modulating the nature of MLN-cDCs, especially R2 and R3.

IL-6 instructs naive T cells to differentiate into IL-13-producing inflammatory Th2 cells

We examined whether IL-6 and other molecules could directly induce IL-13-producing inflammatory Th2 differentiation. In a DC-free culture system, naive CD4⁺ T cells that were

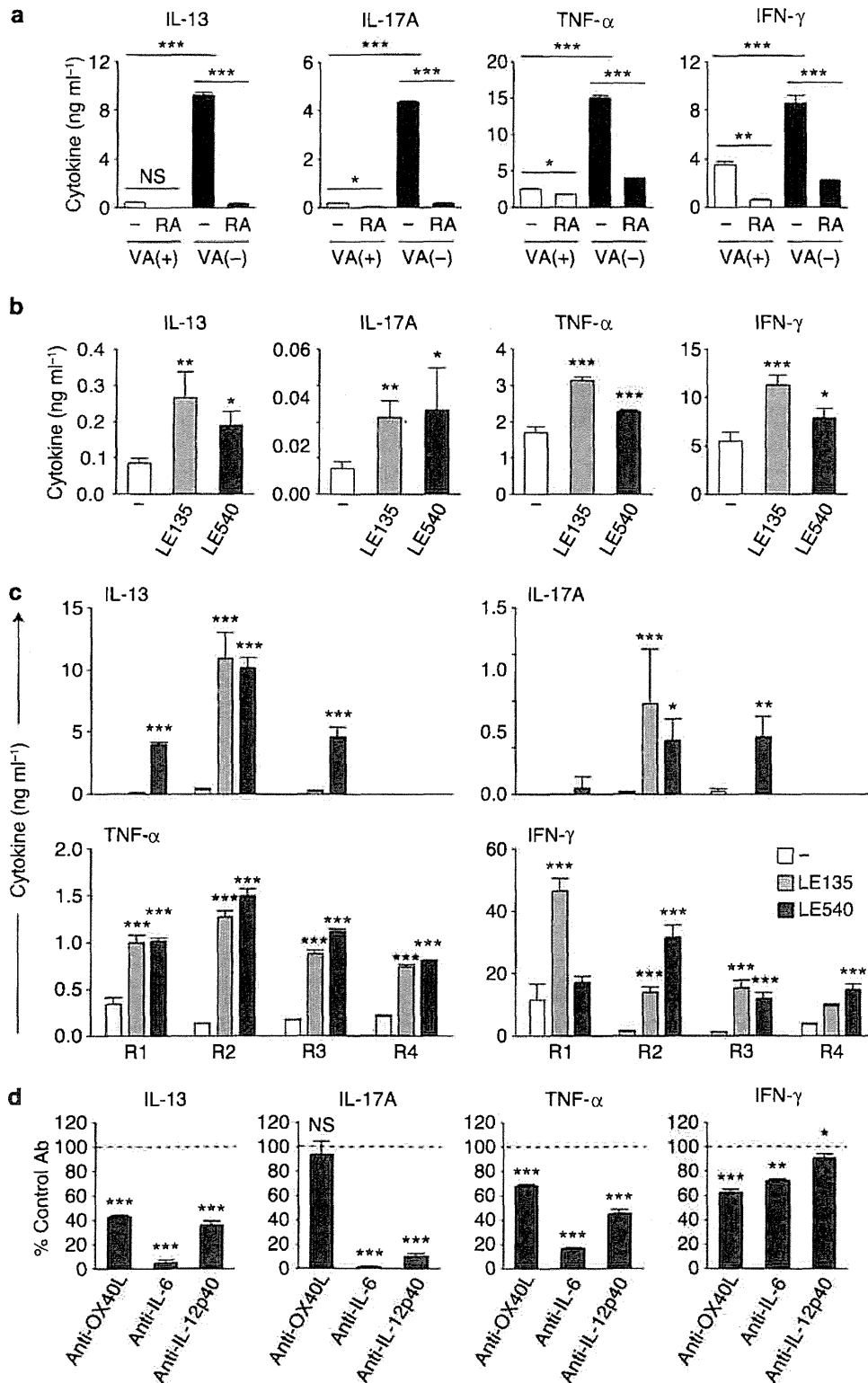


Figure 5 For caption please refer page 791.

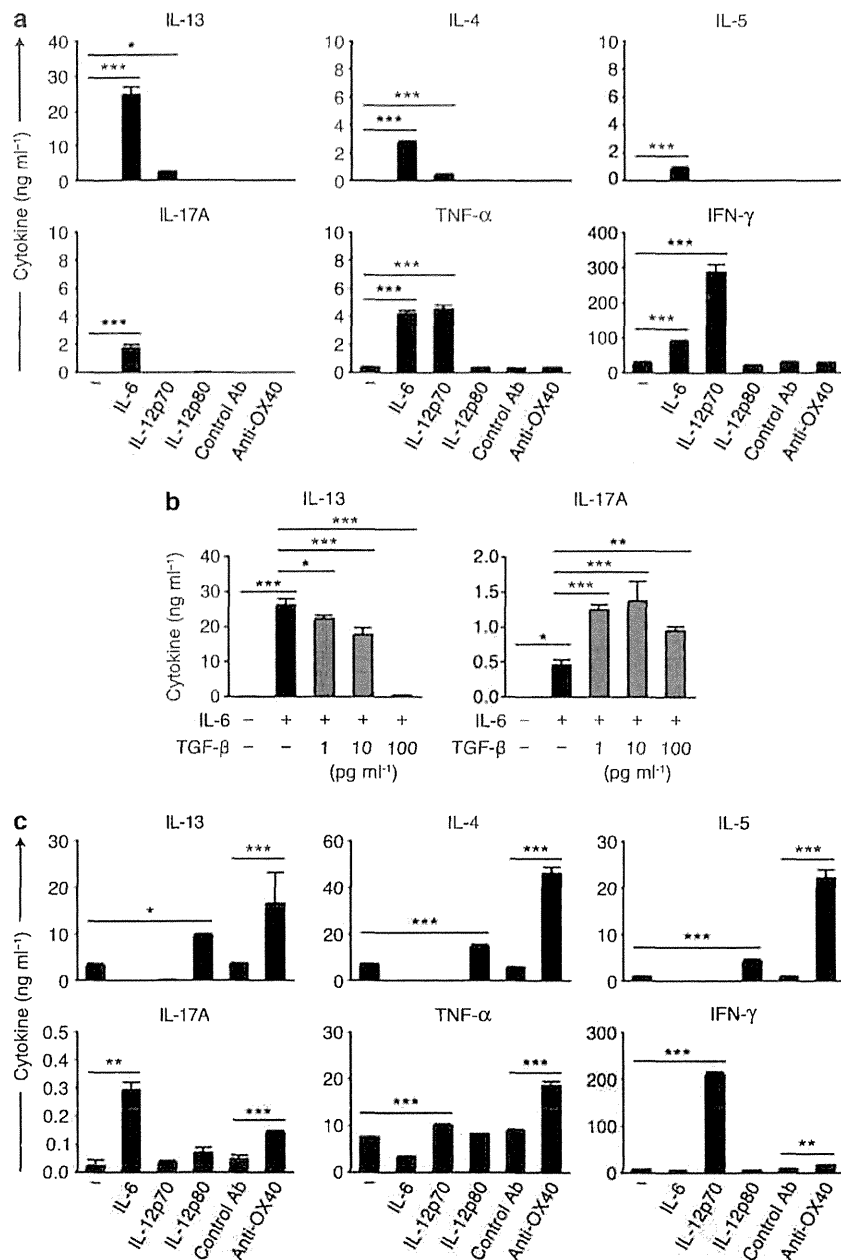


Figure 6 Interleukin-6 (IL-6) instructs naive T cells to differentiate into IL-13-producing inflammatory T helper type 2 (Th2) cells. CD4⁺ T cells from BALB/c mice were stimulated with immobilized monoclonal antibodies (mAbs) to CD3 and CD28 in the presence or absence of (a) IL-6, IL-12p70, IL-12p80 (10 ng ml⁻¹), immobilized agonistic anti-OX40 or Rat IgG1 isotype control mAbs (10 μg ml⁻¹), or (b) IL-6 and/or transforming growth factor-β (TGF-β). The cells were restimulated with immobilized mAbs to CD3 and CD28, and cytokine concentrations in the supernatants were assessed by enzyme-linked immunosorbent assay (ELISA). (c) CD4⁺ T cells from DO11.10/*Rag2*^{-/-} mice were stimulated with ovalbumin peptide and dendritic cells of mesenteric lymph nodes (MLNs) from normal mice in the presence or absence of IL-6, IL-12p70, IL-12p80 (10 ng ml⁻¹), soluble anti-OX40, or Rat IgG1 isotype control mAbs (10 μg ml⁻¹), and were restimulated with immobilized mAbs to CD3 and CD28. Cytokine concentrations in the supernatants were assessed ELISA. Data are presented as mean + s.d. of triplicate samples. **P* < 0.05; ***P* < 0.01; ****P* < 0.001. Similar results were obtained from three independent experiments.

stimulated with antibodies against CD3 and CD28 in the presence of IL-6 differentiated into T cells that produced high levels of IL-13 and TNF-α, and lower levels of IL-17A, IL-4, and IL-5 (Figure 6a). IL-6 also enhanced the induction of IFN-γ-producing T cells but was much less efficient than IL-12p70. On the other hand, TGF-β inhibited the IL-6-dependent induction of IL-13-producing T cells, but reciprocally enhanced the

induction of IL-17A-producing T cells (Figure 6b). Similar results were obtained with naive CD4⁺ T cells of C57BL/6 mice (Supplementary Figure S3). A plate-bound agonistic anti-OX40 antibody failed to affect T-cell cytokine production. However, the anti-OX40 antibody facilitated normal MLN-DCs to induce T cells that produced high levels of IL-4, IL-5, IL-13, and TNF-α (Figure 6c). IL-12p80 moderately

facilitated MLN-DCs to induce Th2 cells. However, the addition of IL-6 rather suppressed the induction of IL-13-producing T cells, and enhanced the induction of IL-17A-producing T cells. TGF- β from MLN-DCs may contribute to this result. These findings collectively suggest that IL-6-dependent signals are essential for the specific induction of IL-13-producing inflammatory Th2 and that TGF- β can regulate IL-13-producing inflammatory Th2 induction. On the other hand, OX40-mediated signals and IL-12p80 likely contribute to skew T cells toward general inflammatory Th2 or Th2-related cell subsets, including IL-13-producing inflammatory Th2.

Proximal colon epithelial cells in VA-deficient mice produce TNF- α that can instruct DCs to express OX40L

VA deficiency also affects the nature of intestinal epithelial cells, and can direct them to produce inflammatory cytokines that induce OX40L expression in DCs.^{32,34,35} Indeed, VA deficiency markedly enhanced TNF- α expression in proximal colon epithelial cells (Figure 7a,b). As lymph from the proximal colon drains into the MLNs, TNF- α production may affect the nature of MLN-DCs. TNF- α induced the expression of OX40L, CD40, and CD86 in murine fms-related tyrosine kinase 3 ligand (Flt3L)-generated bone marrow (BM)-DCs and the production of low levels of IL-6, and RA partly suppressed this induction except for CD40 and IL-6 (Figure 7c,d). TNF- α -treated BM-DCs instructed T cells to produce extremely high levels of IL-4, IL-5, and IL-13 in an OX40L-dependent manner (Figure 7e and f). RA partly suppressed this production. Thus, in VA(-) mice, TNF- α may enhance the ability of MLN-DCs to induce general inflammatory Th2 cells. Accordingly, injections of anti-TNF- α antibody into VA(-) mice for 2 weeks tended to downregulate this ability (data not shown). These results suggest that VA or RA can also regulate the nature of MLN-DCs by suppressing both TNF- α production in the proximal colon and TNF- α signaling in MLN-DCs.

IL-33-expressing cells and thymic stromal lymphopoietin-expressing cells were detected in the MLNs, PPs, small intestine, and proximal colon of unprimed VA(-) mice as frequently as that in VA(+) mice. However, VA deficiency increased the number of IL-33-expressing epidermal cells in the ear (data not shown). IL-33, but not thymic stromal lymphopoietin, induced the CD86, IL-6, and low levels of OX40L and CD40 expression in BM-DCs, and RA partly suppressed this induction (Supplementary Figure S4 and data not shown).

VA deficiency increases the risk of strong immune responses to oral antigens

As MLN-DCs can present oral antigens, we re-examined whether VA deficiency affected oral tolerance, using a classical system of tolerance induction. Mice received repeated intragastric administration of ovalbumin (OVA), followed by challenges of OVA with an adjuvant. In VA(+) mice, regardless of the route of challenge, repeated OVA administration significantly reduced the OVA-induced proliferation of draining MLN or PLN cells *in vitro* compared with saline administration (Figure 8a-c). In VA(-) mice, however,

repeated OVA administration did not significantly reduce cell proliferation (Figure 8a-c), except for PLN-cell proliferation when assessed 1 week after the subcutaneous challenge (Figure 8c, left). The latter result agreed with a previous observation under similar conditions.²² However, PLN cells obtained from OVA-fed VA(-) mice 2 weeks after the subcutaneous challenge proliferated equally to those obtained from saline-fed control mice (Figure 8c, right) as reported previously.¹⁷ Unexpectedly, however, MLN cells obtained from OVA-fed VA(-) mice 1 week after intraperitoneal (i.p.) challenge exhibited higher proliferation levels than those from saline-fed control mice (Figure 8a). After repeated OVA feeding, CD4⁺ T cells from the MLNs and SPLs of VA(-) mice, but not VA(+) mice, produced significant levels of IL-13 and IL-17A upon antigenic stimulation (Figure 8d), indicating that antigen feeding can induce antigen-specific IL-13-producing T cells and IL-17A-producing T cells in VA(-) mice.

Repeated oral antigen administration primes strong antibody responses

In VA(+) mice, OVA feeding suppressed the serum and fecal antibody responses after two i.p. challenges as expected (Figure 9a,b). However, OVA-fed VA(-) mice exhibited aberrantly high serum levels of anti-OVA IgG1 and IgG2a responses (Figure 9a). The total IgG1 and IgG2a concentrations in the sera of these mice reached 6–10 mg ml⁻¹ and 2.0–2.2 mg ml⁻¹, respectively. The anti-OVA IgA levels in the sera of these mice were also significantly higher than those in OVA-fed VA(+) or saline-fed VA(-) mice. Furthermore, significant anti-OVA IgE responses were induced in OVA-fed VA(-) mice. In these mice, a single intradermal OVA injection elicited ear swelling that peaked at ~6 h after the OVA challenge (Figure 9c,d), suggesting that IgE-mediated and mast cell-dependent immediate-type allergic inflammation was induced. Two i.p. challenges, however, spontaneously induced deaths in some VA(-) mice. Elevated antibody responses in the OVA-fed VA(-) mice were already observed after the first i.p. challenge (Supplementary Figure S5). These results suggest that repeated oral antigen administration strongly primes VA(-) mice for antigen-specific antibody responses, especially IgG1 responses, and eventual IgE responses that cause allergic skin inflammation. In saline-fed control mice, however, VA deficiency suppressed the OVA-specific serum antibody and fecal IgA antibody responses, as expected (Figure 9a,b). Fecal anti-OVA IgG1 antibodies were detected in OVA-fed VA(-) mice (Figure 9b), suggesting that the intestinal mucosal barrier functions were reduced in VA(-) mice after repeated antigen administration.

IL-13 is essential for anti-OVA IgG1, IgA, and IgE antibody responses in OVA-pre-fed VA(-) mice

IL-13 and IL-21 promote IgG1 antibody production, whereas IL-17A and IL-21 promote IgG2a antibody production.^{36,37} Thus, IL-13-producing inflammatory Th2 or Th17 cells may contribute to oral antigen-specific IgG1 and IgG2a antibody responses. To examine the role of IL-13 in antibody responses, sera were obtained from *Il13*^{-/-} VA(-) mice after repeated

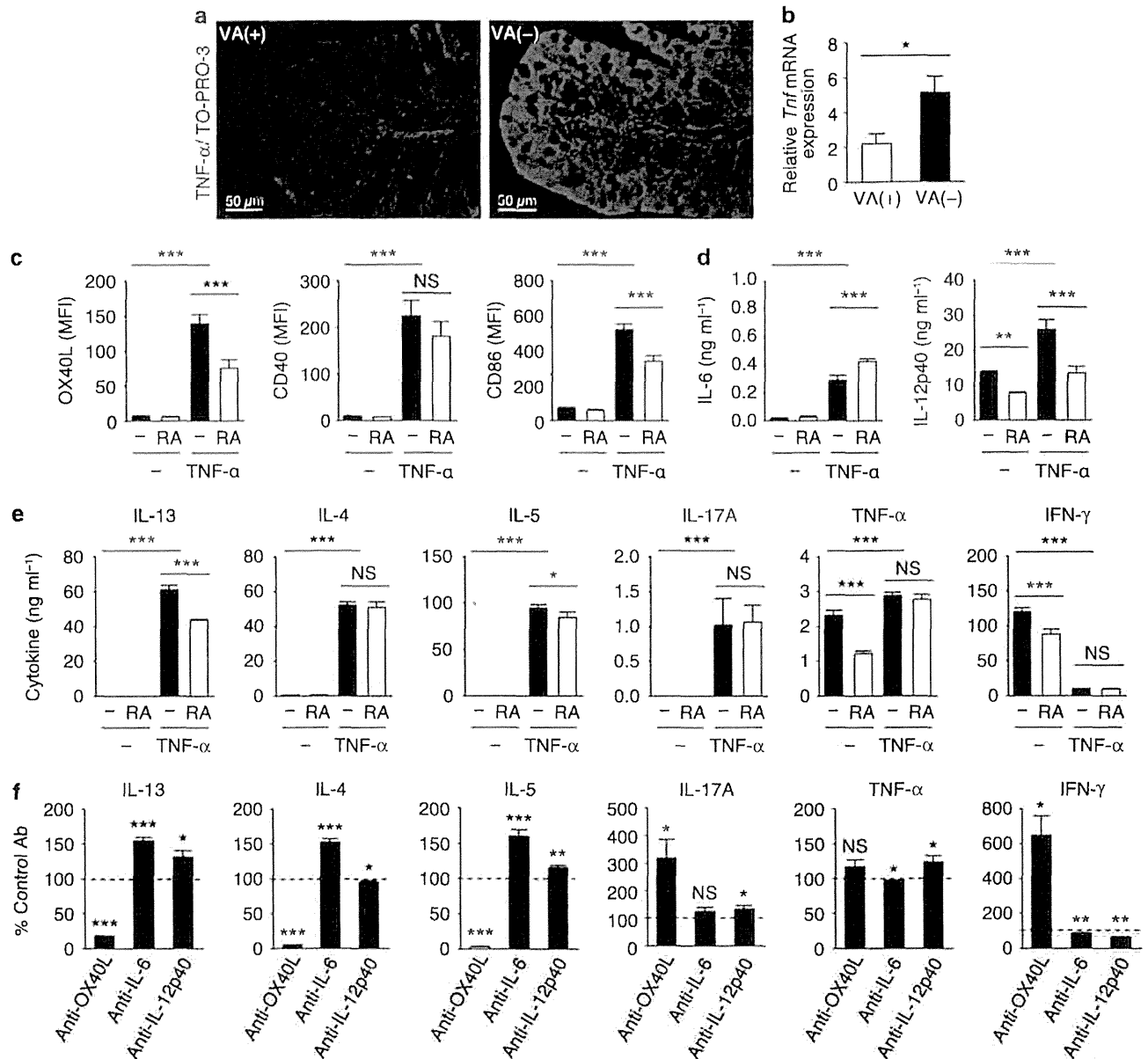


Figure 7 Proximal colon epithelial cells in vitamin (VA)-deficient mice produce tumor necrosis factor- α (TNF- α) that can instruct bone marrow-derived dendritic cells (BM-DCs) to express OX40L and induce general inflammatory T helper type 2 (Th2) cells. (a) Representative immunofluorescence micrographs of TNF- α expression (red) in proximal colons from VA(+) and VA(-) mice ($n=4$ mice/group). Cell nuclei were visualized with TO-PRO-3 (blue). (b) Relative *Tnf* mRNA expression in proximal colon epithelial cells from VA(+) and VA(-) mice ($n=5$ mice/group). Data are presented as mean \pm s.e.m. for each group. * $P < 0.05$. (c-e) BM-DCs generated by fms-related tyrosine kinase 3 ligand were treated with TNF- α in the presence or absence of retinoic acid (RA). (c) Expression levels of costimulatory molecules on the treated BM-DCs were analyzed by flow cytometry. Data are expressed as mean fluorescence intensities (MFIs). (d) Cytokine concentrations in the supernatants were assessed by enzyme-linked immunosorbent assay (ELISA). (e) CD4⁺ T cells from DO11.10/*Rag2*^{-/-} mice were stimulated with ovalbumin (OVA) peptide and the treated BM-DCs, and were restimulated with immobilized monoclonal antibodies (mAbs) to CD3 and CD28. Cytokine concentrations in the supernatants were assessed by ELISA. (f) CD4⁺ T cells were stimulated with OVA peptide and the treated BM-DCs in the presence of anti-OX40L, anti-IL-6, anti-IL-12p40, or isotype control mAbs, and were restimulated with immobilized mAbs to CD3 and CD28. Cytokine concentrations in the supernatants were assessed by ELISA. Results are shown as the percentage of the control culture with the isotype control mAb. * $P < 0.05$; ** $P < 0.01$; *** $P < 0.001$; NS, not significant vs. control mAb. Data are presented as mean \pm s.d. of quadruplicate samples. Representative results from three independent experiments are shown.

OVA administration, followed by oral challenges. The observed anti-OVA IgG1, IgA, and IgE responses were low (Figure 10a). On the other hand, *Il13* deficiency did not affect anti-OVA IgG2a responses. Similar results, with stronger responses, were obtained from mice that received i.p. challenges with alum (data not shown). The results suggest that in VA(-) mice, IL-13 is

essential to enhance IgG1, IgA, and IgE responses but not IgG2a responses. OVA prefeeding suppressed the OVA-induced proliferation of MLN cells from VA(+) and VA(-) *Il13*^{-/-} mice that received intragastric OVA administration and adjuvant (Figure 10b), suggesting that IL-13 is not required for the induction of oral tolerance in T cells of VA(+) mice, but

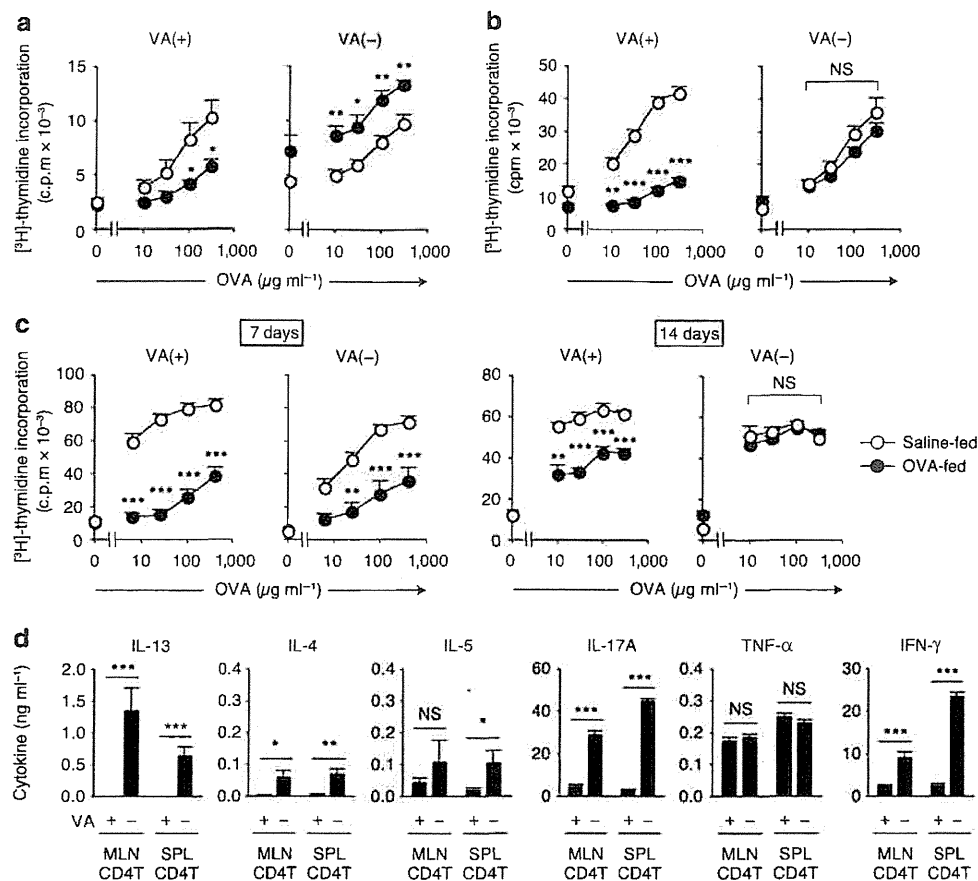


Figure 8 Vitamin A (VA) deficiency compromises oral tolerance induction. VA(+) and VA(-) mice were fed with ovalbumin (OVA) or saline every other day for a total of five times. (a, b) OVA- or saline-fed mice were (a) immunized intraperitoneally with 0.1 mg of OVA in alum ($n=6-7$ mice/group) or (b) immunized intragastrically with 10 mg of OVA plus cholera toxin ($n=4$ mice/group) 7 days after the last feeding. OVA-specific proliferation of draining mesenteric lymph node (MLN) cells was assessed 7 days after immunization. (c) OVA- or saline-fed mice were immunized subcutaneously with 0.1 mg of OVA in complete Freund's adjuvant 7 days after the last feeding. OVA-specific proliferation of draining peripheral lymph node cells was assessed 7 or 14 days after immunization ($n=4-5$ mice/group). Data are presented as mean + s.e.m. for each group. * $P<0.05$; ** $P<0.01$; *** $P<0.001$; NS, not significant vs. treatment with the same concentration of OVA. (d) CD4⁺ cells were obtained from MLNs and spleens (SPLs) of OVA- or saline-fed mice without subsequent immunization 24 h after the last feeding. The cells were cultured with irradiated SPL cells and OVA for 3 days, and cytokine levels in the culture supernatants were assessed by enzyme-linked immunosorbent assay (ELISA). Data are presented as mean + s.d. of quadruplicate samples. Representative results from (a, d) four or (b, c) two independent experiments are shown.

is essential for the disruption of oral tolerance in T cells of VA(-) mice.

DISCUSSION

VA deficiency affects the nature of MLN-DCs even in unprimed mice. In particular, the CD8 α ⁻CD11b⁺CD103⁻cDC (R2) subset of VA(-)MLN-DCs exhibited the ability to instruct naive CD4⁺ T cells to differentiate into IL-13-producing inflammatory Th2 cells in an IL-6-dependent manner. IL-6 alone efficiently induced IL-13-producing inflammatory Th2 cells from naive CD4⁺ T cells upon activation with antibodies to CD3 and CD28, indicating that IL-6-mediated signaling is essential and sufficient for IL-13-producing inflammatory Th2 induction in the absence of DCs. TGF- β 1 downregulated IL-13-producing inflammatory Th2 induction, and reciprocally upregulated Th17 induction, suggesting that TGF- β levels in the

microenvironment regulate the IL-13-producing inflammatory Th2/Th17 balance.

OX40/OX40L-mediated signaling also appeared to participate in IL-13-producing inflammatory Th2 induction by enhancing the generation of general inflammatory Th2 cells and suppressing that of Th17 cells. VA(-)MLN-DCs expressed much higher levels of *Tnfrsf4* than VA(+)MLN-DCs. However, among VA(-)MLN-DCs, the R3 subset expressed higher levels of *Tnfrsf4* than R2, despite the fact that R2 induced IL-13-producing inflammatory Th2 more efficiently than R3. An agonistic anti-OX40 antibody affected IL-13-producing inflammatory Th2/Th17 balance in the presence of MLN-DCs, suggesting that T cell/DC interactions mediated by other molecules could also be involved. In VA(-) mice, TNF- α produced by epithelial cells in the proximal colon may flow into the draining MLNs and partly contribute to the induction of inflammatory Th2 cells by enhancing OX40L expression in MLN-DCs, although further analysis is necessary.

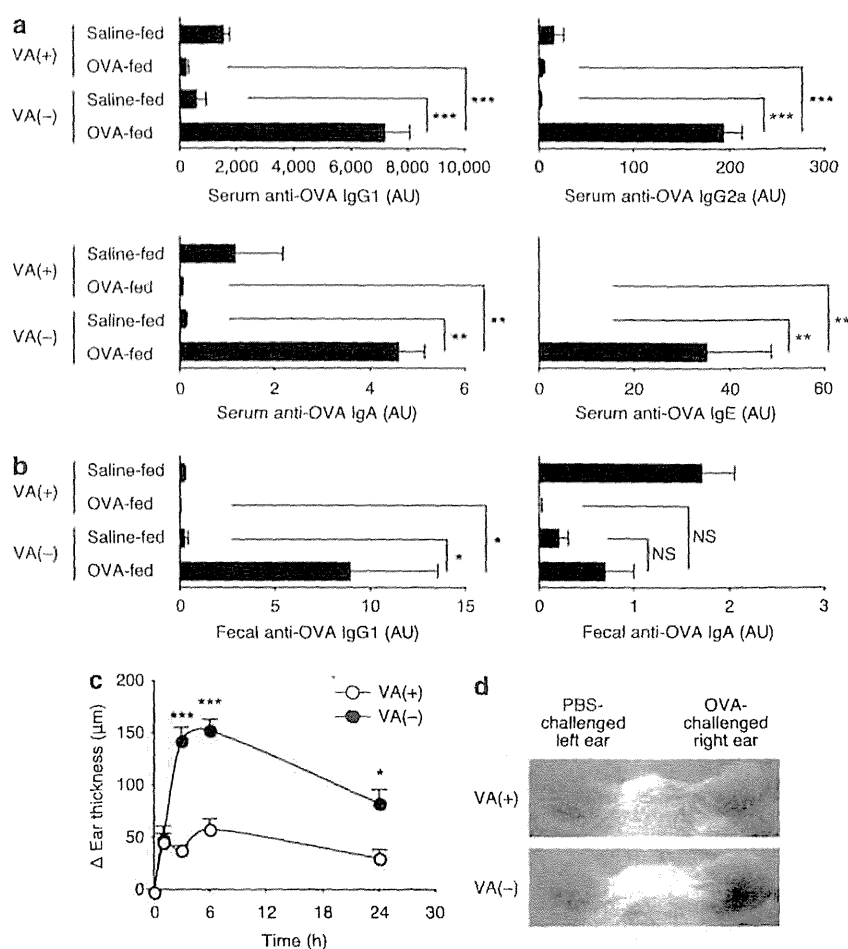


Figure 9 Repeated oral administration of ovalbumin (OVA) to vitamin A-deficient (VA(-)) mice primes for strong antibody responses. (a, b) OVA- or saline-fed VA(+) and VA(-) mice ($n=5$ mice/group) were immunized intraperitoneally (i.p.) with 0.1 mg of OVA in alum 7 and 21 days after the last feeding. (a) The serum samples and (b) the fecal extracts were prepared 7 days after the last immunization, and were assessed by enzyme-linked immunosorbent assay (ELISA) for OVA-specific antibodies ($n=5$ VA(+) and $n=3$ VA(-) mice/group, two out of five OVA-fed or saline-fed VA(-) mice were dead after the second immunization). The antibody levels were defined by comparing with standard serum and expressed in arbitrary units (AU). Data are presented as mean \pm s.e.m. for each group. * $P<0.05$; ** $P<0.01$; *** $P<0.001$; NS, not significant. IgG1, immunoglobulin G1. (c) Ear thickness of OVA-fed and i.p. immunized mice was measured at the indicated time points after intradermal injection of 10 μ g of OVA into the right ear and phosphate-buffered saline (PBS) into the left ear. The differences between right and left ear thickness (Δ ear thickness) are presented as mean \pm s.e.m., $n=4$ mice/group. * $P<0.05$; *** $P<0.001$. (d) Representative photographs of the ears taken 6 h after intradermal injection. Similar results were obtained from two independent experiments.

IL-12p40 also appeared to participate in the R2-mediated generation of IL-13-producing inflammatory Th2 but not Th17 cells. The homodimer IL-12p80 inhibits IL-12-mediated responses and contributes to Th2-type allergic diarrhea.³⁸ Accordingly, IL-12p80 moderately enhanced Th2 induction. Th1-derived IFN- γ is known to suppress both Th2 and Th17 differentiation.³⁹ Interestingly, CD103⁺ MLN-DCs of VA(-) mice produce IFN- γ upon stimulation.⁴⁰ IFN- γ may contribute to the difference in the nature of R2 and R3. The nature of R3 may also be influenced by CD103⁺ langerin⁺ immunosuppressive DCs, which are found in VA(-) MLNs.²² R2- and R3-stimulated T cells produced low levels of IL-4, but these levels may still influence general Th2 skewing.

IL-13-producing inflammatory Th2 and Th17 may also influence each other. IL-13 attenuates Th17 cytokine production.⁴¹ However, IL-17A enhances downstream IL-13 signals.⁴²

IL-13 appeared to be essential for the aberrant proliferation of T cells from VA(-) mice. The underlying mechanism remains to be clarified, but IL-13-producing inflammatory Th2 may have been the major influence on proliferating T cells in the MLN culture or could have induced IL-13-producing inflammatory Th2 proliferation in an autocrine manner. The complex interplay of cytokines is likely to influence IL-13-producing inflammatory Th2 induction.

IL-13-producing inflammatory Th2 cells induced by VA(-) MLN-DCs expressed homing receptors for inflammatory sites or the skin. Indeed, these cells could migrate into inflamed skin. In VA(-) animals, the administration of food and bacterial antigens to the skin could thus pose a risk of IL-13-producing inflammatory Th2-dependent inflammation. IL-13-producing inflammatory Th2 cells that are primed in the MLNs could induce antigen-specific inflammatory responses in any tissues

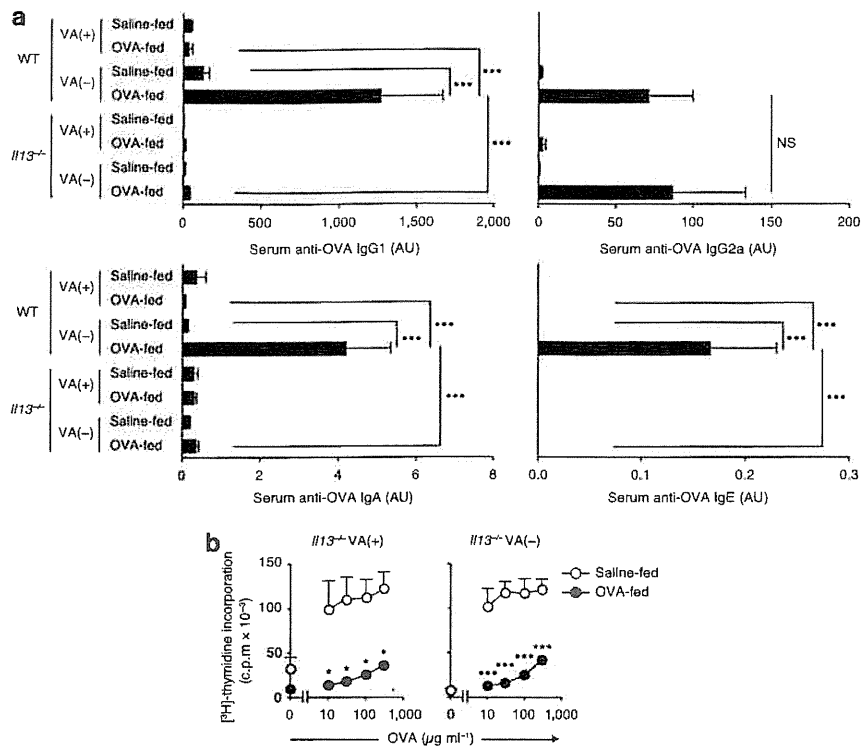


Figure 10 Interleukin-13 (IL-13) is essential for the enhanced anti-ovalbumin (OVA) antibody responses in vitamin A-deficient (VA(-)) mice after OVA feeding. **(a)** OVA- or saline-fed wild-type (WT) VA(+), WT VA(-), *Il13*^{-/-} VA(+), and *Il13*^{-/-} VA(-) mice ($n=4-7$ mice/group) were immunized intragastrically with 10 mg of OVA plus cholera toxin 7, 14, and 21 days after the last feeding. The serum samples were prepared 7 days after the last immunization assessed by enzyme-linked immunosorbent assay for OVA-specific antibodies. The antibody levels were defined by comparing with standard serum and expressed in arbitrary units (AU). Data are presented as mean + s.e.m. for each group. *** $P<0.001$. Representative results from three independent experiments are shown. IgG1, immunoglobulin G1. **(b)** OVA- or saline-fed *Il13*^{-/-} VA(+) and *Il13*^{-/-} VA(-) mice were immunized intragastrically with 10 mg of OVA plus cholera toxin 7 days after the last feeding. OVA-specific proliferation of draining mesenteric lymph node (MLN) cells was assessed 7 days after immunization. Data are presented as mean + s.e.m., 4 mice/group. * $P<0.05$; *** $P<0.001$.

with innate inflammation and blood-borne antigens that could be increased with repeated oral antigen administration or an infectious gut insult under VA(-) conditions.⁴³ Reductions in endogenous RA or VA concentrations have been observed in atopic dermatitis and other inflammatory diseases.^{44,45} Inflammatory Th2 cells often participate in these diseases. On the other hand, VA or RA treatment ameliorates various inflammatory diseases.⁴⁶ IL-13 is known to play central roles in asthma.²⁴⁻²⁷ As CCR4 contributes to T-cell lung imprinting,⁴⁷ IL-13-producing inflammatory Th2 cells may also be able to contribute to the antigen-specific asthmatic reaction. However, VA deficiency reduced disease severity in a mouse model of asthma induced by i.p. injections of OVA and alum, followed by exposures to aerosolized OVA.⁴⁸ In the absence of OVA feeding, we also observed lower antibody responses in VA(-) mice compared with VA(+) mice. Antigen prefeeding appears to be critical in inducing unusually high antibody responses in VA(-) mice. Nonetheless, relatively low dietary VA intake is known to be associated with asthma.⁴⁹

Strong IgG1 responses and IgE responses were induced against OVA, a T cell-dependent antigen, in VA(-) mice. The IgE levels were sufficient to induce immediate-type allergic responses in the skin. However, previous reports suggested that

VA deficiency reduces antibody responses to T cell-dependent antigens and T cell-independent-type 2 antigens.^{12,13} On the other hand, VA deficiency in rats enhanced bacterial translocation into the MLNs and the serum levels of IgG, IgM, and IgE antibodies against bacterial antigens including the T cell-independent antigen lipopolysaccharide.¹³ Similarly, in unprimed mice, VA deficiency induced the elevation of serum IgG2a and IgG2b levels but not of IgG1, IgG3, or IgA levels.^{10,40} Commensal bacterial antigens such as lipopolysaccharide may contribute to this elevation. The strong IgG1 responses and IgE responses to OVA in the OVA-fed VA(-) mice likely involve OVA-specific IL-13-producing inflammatory Th2 cells induced by VA(-) MLN-DCs. OVA feeding alone induced OVA-specific IL-13-producing CD4⁺ T cells in the MLNs of VA(-) mice. T cell-independent antigens derived from commensal bacteria may facilitate T-cell priming and the induction of antibody responses. Furthermore, additional adjuvant-induced signals may be necessary to trigger or enhance antibody responses.

Foxp3⁺CD103⁺ T cells are present even in mice with low VA levels.⁵⁰ Accordingly, VA(-) PP-DCs induced Foxp3⁺ CD103⁺ T-cell differentiation. The CCR9⁺ PP-pDCs in VA(-) mice may be tolerogenic, as their phenotype resembled

that of tolerogenic CCR9⁺ pDCs.³³ Nonetheless, in VA(−) mice, oral antigen-specific inflammatory effector T cells including IL-13-producing inflammatory Th2 and Th17 appear to overcome the effect of regulatory T cells.

RA is required for immature DCs to express RALDH2.^{6,21,51} Bile retinoids contribute to the induction of RALDH2 expression in lamina propria-DCs and MLN-DCs.⁹ Therefore, liver dysfunction may affect RALDH2 expression in gut CD103⁺ DCs by reducing the production of bile retinoids and other components necessary for the intestinal absorption of lipids including RA precursors. Accordingly, young children with severe liver dysfunction have a high prevalence of food allergies, with specific IgE responses.⁵²

The presence of RAR α appears to be critical for CD4⁺ T-cell activation and differentiation.^{18,53} In VA(−) mice, weak RAR α signaling induced by residual levels of retinol or other molecules may be necessary for inducing inflammatory arms of immunity. Indeed, the retinol levels in our VA(−) mouse sera were <1/10 of the control but not completely absent. Therefore, the present results suggest that VA insufficiency in the gut increases the risk of IL-13-dependent inflammatory or allergic diseases by inducing oral antigen-specific IL-13-producing inflammatory Th2 cells as well as the risk of Th17-dependent diseases by changing the nature of MLN-DCs.

METHODS

Mice. BALB/c, C57BL/6, and DO11.10/*Rag2*^{-/-} mice were obtained from CLEA Japan (Tokyo, Japan) and Taconic (Hudson, NY), respectively. BALB/c *Il13*^{-/-} mice were generated by backcrossing B6x129 *Il13*^{-/-} mice (kindly provided by Dr Andrew McKenzie, MRC Laboratory of Molecular Biology, Cambridge, UK).³⁶ VA(−) and VA(+) mice were generated as previously described.⁶ All mice were maintained in specific pathogen-free conditions in the animal facility of Tokushima Bunri University (Kagawa, Japan). All animal experiments were performed according to protocols approved by the Animal Care and Use Committee of Tokushima Bunri University.

Cell preparation. DCs were isolated by MACS (Miltenyi Biotec, Bergisch Gladbach, Germany) as previously described.⁶ Sorting of DC subsets was performed on a FACSAria (BD, Franklin Lakes, NJ) after staining with fluorochrome-conjugated monoclonal antibodies (mAbs) against CD11c, B220, CD8 α , CD11b, and CD103 (Supplementary Table S1 online). Naive CD4⁺ CD62L^{high} T cells were obtained from lymph nodes and SPLs of DO11.10/*Rag2*^{-/-} mice by negative selection using EasySep Mouse CD4⁺ T Cell Enrichment Kits (Stemcell Technologies, Vancouver, BC, Canada). In some experiments, naive CD4⁺ CD62L^{high} CD44⁻ T cells were obtained from SPLs of BALB/c or C57BL/6 mice by negative selection using EasySep Mouse CD4⁺ T Cell Enrichment Kits supplemented with biotinylated anti-CD44 mAb (IM7; BioLegend, San Diego, CA) and subsequently by positive selection with CD62L Microbeads (Miltenyi Biotec). To isolate proximal colon epithelial cells, the proximal colon was incubated with Hanks' balanced salt solution containing 1 mM dithiothreitol as previously described.⁶ BM-DCs were generated by culturing BM cells for 7 days in the presence of 20% culture supernatant of a mouse Flt3L-transfected CHO cell line, and then stimulated with 50 ng ml⁻¹ TNF- α (Peprotech, Rocky Hill, NJ) or 100 ng ml⁻¹ IL-33 (BioLegend) in the presence or absence of 10 nM all-*trans*-RA for 48 h.

Cell culture. DCs (2–4 \times 10³) were cocultured for 6 days with naive CD4⁺ T cells (1–2 \times 10⁴) from DO11.10/*Rag2*^{-/-} mice in the

presence of OVA peptide P323–339 (1 μ M) with or without all-*trans*-RA (10 nM; Sigma-Aldrich, St Louis, MO), LE135 (100 nM; Tocris Bioscience, Bristol, UK), LE540 (100 nM; Wako, Osaka, Japan), IL-6, IL-12p70, or IL-12p80 (10 ng ml⁻¹; BioLegend). In some experiments, neutralizing anti-IL-6 (MP5-20F3; BioLegend), anti-IL-12p40 (C17.8; BD), anti-IL-23p19 (G23-8; eBioscience, San Diego, CA), or anti-OX40L (182601; R&D Systems, Minneapolis, MN), agonistic anti-OX40 (OX-86; eBioscience), Rat IgG1 isotype control (43414; R&D Systems), or Rat IgG2a isotype control (54447; R&D Systems) were used at 10 μ g ml⁻¹. For induction of regulatory T cells, cultures were supplemented with 5 ng ml⁻¹ TGF- β 1 (Peprotech). For induction of Ccr9 expression in T cells, DCs were pretreated with 1 μ M OVA peptide P323–339 for 2 h, washed, and then cocultured with naive CD4⁺ T cells.⁵⁴ Naive CD4⁺ T cells (1 \times 10⁵) from BALB/c or C57BL/6 mice were cultured for 3 days in the plates coated with anti-CD3 mAb (3 μ g ml⁻¹) and anti-CD28 mAb (3 μ g ml⁻¹) with or without anti-OX40 or Rat IgG1 isotype control (10 μ g ml⁻¹). The culture was diluted with twice its volume of fresh medium, transferred into new wells, and cultured for 3 days. Cytokines were added at the start of each culture. For the experiment in Figure 6b, TGF- β 1 (R&D Systems) was used after reconstituting in 4 mM hydrochloric acid containing 1 mg ml⁻¹ bovine serum according to the manufacturer's protocol. To assess T-cell cytokine production, the cells (1 \times 10⁵) were resuspended and cultured for 3 days in the plates coated with anti-CD3 mAb (3 μ g ml⁻¹) and anti-CD28 mAb (3 μ g ml⁻¹). Cytokine levels in the culture supernatants were analyzed by enzyme-linked immunosorbent assay (ELISA).

Flow cytometry. Cells were stained with fluorochrome-conjugated mAbs (Supplementary Table S1) in the presence of anti-CD16/CD32 mAb (2.4G2; BD). Staining of E- and P-selectin ligands was performed as previously described.⁶ Intracellular staining of Foxp3 was performed using mouse/rat Foxp3 staining sets (eBioscience). For intracellular cytokine staining, CD4⁺ T cells obtained from cultures were restimulated with immobilized anti-CD3 mAb (10 μ g ml⁻¹) and soluble anti-CD28 mAb (5 μ g ml⁻¹) in the presence of monensin (2 μ M) for 6 h. The cells were fixed and permeabilized with Fixation/Permeabilization Buffers (eBioscience), and intracellular cytokine staining was performed according to the manufacturer's protocol. Analysis was performed on a FACSCalibur (BD) or FACSAria with CellQuest Pro software (BD).

Real-time PCR. Total RNA was isolated from cells using RNeasy Kit (Qiagen, Hilden, Germany), and complementary DNA was generated using QuantiTect Reverse Transcription Kit (Qiagen). Complementary DNA was used as a template for real-time PCR in triplicates with Power SYBR Green PCR Master Mix (Applied Biosystems, Foster City, CA) and gene-specific primers (Supplementary Table S2). PCR analyses were performed on a 7500 Real-Time PCR system (Applied Biosystems). The expression of each gene was normalized with *Rplp0*, and relative expression was quantified with the 2^{- Δ Ct} value multiplied by 1,000.

Homing assay. CD4⁺ DO11.10/*Rag2*^{-/-} T cells activated with VA(+)MLN-DCs or VA(−)MLN-DCs were differentially labeled with 5-chloromethylfluorescein diacetate and SNARF[®]-1 carboxylic acid acetate succinimidyl ester (Life Technologies, Carlsbad, CA) as previously described.⁵⁵ An aliquot (2–3 \times 10⁷) of the cells was injected intravenously into each BALB/c mouse with preexisting cutaneous inflammation in both ears induced by a standard delayed hypersensitivity protocol as previously described³¹ with modification. In brief, shaved abdomens of the mice were painted with 50 μ l 0.5% 2,4-dinitro-1-fluorobenzene (Nacalai tesque, Kyoto, Japan) in acetone/olive oil (4:1) on day 0. On day 5, mice were challenged with 20 μ l 0.3% 2,4-dinitro-1-fluorobenzene on both ears, and used on the next day as recipients for competitive homing experiments. Recipients were killed 16 h after the adoptive transfer, and the transferred cells were recovered from MLNs and both ears after digestion with collagenase

type VIII (Sigma-Aldrich). To assess the migration efficiency of the transferred cells, the ratios of SNARF-1⁺ cells/CMFDA⁺ cells in recipient tissues were analyzed by flow cytometry.

Immunohistochemical analysis. MLNs, tissue blocks of the small intestine with PP, proximal colon, and ear from VA(+) and VA(-) mice were immersion-fixed in 4% paraformaldehyde in 0.1 M phosphate buffer (pH 7.2). The fixed tissues were immersed in 20% sucrose in 0.1 M phosphate buffer overnight for cryoprotection, embedded in O.C.T. compound (Sakura Finetek Japan, Tokyo, Japan), and then frozen on dry ice. Frozen sections (8 µm thick) of these tissues were cut out and thaw-mounted onto silane-coated glass slides. These sections were blocked with 5% normal donkey serum (Jackson ImmunoResearch, West Grove, PA) for 1 h at room temperature. The sections were incubated with rabbit anti-TNF-α (Abcam, Cambridge, MA) at 4°C for at least 48 h followed by the incubation with Cy3-conjugated donkey anti-rabbit IgG (Jackson ImmunoResearch) for 1 h at room temperature. TO-PRO-3 (Molecular Probes, Eugene, OR) was used for nuclear staining. Immunostained sections were coverslipped with glycerol and observed using a confocal laser scanning microscopy (FV-1000; Olympus, Tokyo, Japan).

Induction of oral tolerance and immunization. Mice were fed 10 mg of OVA (grade V; Sigma-Aldrich) or saline alone by gavage 5 times every other day (on days 0, 2, 4, 6, and 8). The mice were immunized with 0.1 mg of OVA in adjuvant (2 mg of Imject Alum (Thermo Fisher Scientific, Waltham, MA) for i.p., or complete Freund's adjuvant (Sigma-Aldrich) for subcutaneous administration) 7 days after the last feeding (day 15). In some experiments, the mice were immunized intragastrically with 10 mg of OVA and 10 µg of cholera toxin (List Biological Laboratories, Campbell, CA). OVA-specific proliferation of draining lymph node cells was assessed 7 or 14 days after immunization (day 22 or 29). To assess antibody responses, OVA- or saline-fed mice were immunized i.p. with 0.1 mg of OVA in alum 7 and 21 days after the last feeding (on days 15 and 29), whereas the other mice were immunized intragastrically with 10 mg of OVA plus cholera toxin 7, 14, and 21 days after the last feeding (on days 15, 22, and 29). The serum and the rectal feces of each mouse were collected 7 days after the last immunization (day 36). Feces were adjusted to a 100 mg ml⁻¹ concentration in phosphate-buffered saline containing protease inhibitors (Complete, Mini; Roche Applied Science, Indianapolis, IN) and 0.1% sodium azide. The feces were homogenized, incubated for 1 h on ice, and centrifuged for 15 min at 20,000 g to remove solid material. To assess CD4⁺ T-cell cytokine production, MLNs and SPLs were obtained from the OVA- or saline-fed mice without subsequent immunization 24 h after the last feeding. CD4⁺ cells were isolated by positive selection with CD4 Microbeads (Miltenyi Biotec). Aliquots (4 × 10⁵) were cultured with irradiated SPL cells (1 × 10⁶) and OVA (1 mg ml⁻¹) for 3 days. Cytokine levels in the culture supernatants were analyzed by ELISA.

Antigen-induced ear swelling assay. VA(+) and VA(-) mice fed OVA 5 times were immunized with two i.p. injections of OVA/alum as described above. At 7 days after the last immunization, the left ears of mice were intradermally administered with 10 µg of OVA in 10 µl of phosphate-buffered saline, and their right ears were administered an equal amount of phosphate-buffered saline by using a microsyringe (1701LT; Hamilton, Reno, NV). Ear thickness was measured with a dial thickness gage (No. 7331; Mitsutoyo, Kanagawa, Japan).

Proliferation assay. Single-cell suspensions were prepared from draining MLNs or PLNs (inguinal and popliteal lymph nodes) of individual mice and cultured at 5 × 10⁵ cells with graded concentrations of OVA for 4 days. The cells were pulsed with 1 µCi of [³H]-thymidine for the last 16 h of culture and their radioactivity was counted on a 1450 Microbeta TriLux (PerkinElmer, Waltham, MA).

ELISA. Cytokine levels in the culture supernatants were analyzed with ELISA kits for IFN-γ, IL-4, IL-5, IL-6, IL-10, IL-12p40, IL-12p70,

TNF-α (BD), IL-9, IL-17A, IL-23p19 (BioLegend), IL-13, and IL-21 (R&D Systems). To detect OVA-specific antibodies, plates were coated with 20 mg ml⁻¹ OVA in 0.05 M carbonate-bicarbonate buffer (pH 9.6), and blocked with 5% normal goat serum (Sigma-Aldrich) in Tris-buffered saline. Serially diluted serum samples or fecal extracts and standard serum (pooled hyperimmune sera collected after i.p. immunization with 0.1 mg of OVA in alum 3 times at 2-week intervals) were added and incubated for 2 h. After washing, horseradish peroxidase-conjugated goat anti-mouse IgG1, IgG2a, or IgA (Bethyl Laboratories, Montgomery, TX) were added and incubated for 1 h. To detect anti-OVA IgE, biotinylated anti-mouse IgE (BioLegend) was added for 1 h, followed by addition of horseradish peroxidase-conjugated avidin (BioLegend). The reactions were developed with 3,3',5,5'-tetramethylbenzidine substrate (Sigma-Aldrich) and stopped with 1 M H₂SO₄. The absorbance at 450 nm was measured using a microplate reader (Bio-Rad Laboratories, Hercules, CA). OVA-specific antibody levels were defined by comparing with standard serum and expressed in arbitrary units (AU). Total antibodies were analyzed with ELISA kits for mouse IgG1, IgG2a, IgA (Bethyl Laboratories), and IgE (BioLegend).

Statistical analysis. Statistical comparisons were carried out using the one-way analysis of variance with Tukey-Kramer multiple comparisons test and the two-tailed unpaired Student's *t*-test. Values <0.05 were considered statistically significant.

SUPPLEMENTARY MATERIAL is linked to the online version of the paper at <http://www.nature.com/mi>

ACKNOWLEDGMENTS

We thank Dr A.N.J. McKenzie for B6x129//13 mice, Dr M. Murakami for Flt3L-transfected CHO cell line, Dr K. Ishizaka for critical reading of the manuscript, Dr M. Kubo for intracellular IL-13-staining method, and Ms N. Uemura, H. Tanihigashi-Hayase, and M. Oda for technical assistance. This work was supported by a Grant-in-Aid for Young Scientists (B) (to A.Y.-N.), grants from Uehara Memorial Foundation (to M.I.), The Danone Institute of Japan Research Grant (to M.I.), and JST, CREST (to M.I.), and a Grant-in-Aid for Scientific Research (B) from the Ministry of Education, Science, Sports and Culture of Japan (to M.I.).

DISCLOSURE

The authors declared no conflict of interest.

© 2014 Society for Mucosal Immunology

REFERENCES

1. Imdad, A., Yakoob, M.Y., Sudfeld, C., Haider, B.A., Black, R.E. & Bhutta, Z.A. Impact of vitamin A supplementation on infant and childhood mortality. *BMC Public Health* 11 (Suppl 3), S20 (2011)2011).
2. Hofmann, A.F. The continuing importance of bile acids in liver and intestinal disease. *Arch. Intern. Med.* 159, 2647–2658 (1999).
3. Laffont, S., Siddiqui, K.R. & Powrie, F. Intestinal inflammation abrogates the tolerogenic properties of MLN CD103⁺ dendritic cells. *Eur. J. Immunol.* 40, 1877–1883 (2010).
4. Clugston, R.D. & Blaner, W.S. The adverse effects of alcohol on vitamin A metabolism. *Nutrients* 4, 356–371 (2012).
5. Iwata, M., Hirakiyama, A., Eshima, Y., Kagechika, H., Kato, C. & Song, S.Y. Retinoic acid imprints gut-homing specificity on T cells. *Immunity* 21, 527–538 (2004).
6. Yokota, A. *et al.* GM-CSF and IL-4 synergistically trigger dendritic cells to acquire retinoic acid-producing capacity. *Int. Immunol.* 21, 361–377 (2009).
7. Coombes, J.L. *et al.* A functionally specialized population of mucosal CD103⁺ DCs induces Foxp3⁺ regulatory T cells via a TGF-β and retinoic acid-dependent mechanism. *J. Exp. Med.* 204, 1757–1764 (2007).
8. Sun, C.M. *et al.* Small intestine lamina propria dendritic cells promote de novo generation of Foxp3 T reg cells via retinoic acid. *J. Exp. Med.* 204, 1775–1785 (2007).

9. Jaensson-Gyllenback, E. *et al.* Bile retinoids imprint intestinal CD103⁺ dendritic cells with the ability to generate gut-tropic T cells. *Mucosal Immunol.* **4**, 438–447 (2011).
10. Mora, J.R. *et al.* Generation of gut-homing IgA-secreting B cells by intestinal dendritic cells. *Science* **314**, 1157–1160 (2006).
11. Iwata, M. & Yokota, A. Retinoic acid production by intestinal dendritic cells. *Vitam. Horm.* **86**, 127–152 (2011).
12. Ross, A.C., Chen, Q. & Ma, Y. Augmentation of antibody responses by retinoic acid and costimulatory molecules. *Semin. Immunol.* **21**, 42–50 (2009).
13. Wiedermann, U., Hanson, L.A., Bremell, T., Kahu, H. & Dahlgren, U.J. Increased translocation of *Escherichia coli* and development of arthritis in vitamin A-deficient rats. *Infect. Immun.* **63**, 3062–3068 (1995).
14. Mucida, D. *et al.* Reciprocal Th₁₇ and regulatory T cell differentiation mediated by retinoic acid. *Science* **317**, 256–260 (2007).
15. Curotto de Lafaille, M.A., Kutchukhidze, N., Shen, S., Ding, Y., Yee, H. & Lafaille, J.J. Adaptive Foxp3⁺ regulatory T cell-dependent and -independent control of allergic inflammation. *Immunity* **29**, 114–126 (2008).
16. Hadis, U. *et al.* Intestinal tolerance requires gut homing and expansion of FoxP3⁺ regulatory T cells in the lamina propria. *Immunity* **34**, 237–246 (2011).
17. Cassani, B. *et al.* Gut-tropic T cells that express integrin $\alpha 4\beta 7$ and CCR9 are required for induction of oral immune tolerance in mice. *Gastroenterology* **141**, 2109–2118 (2011).
18. Hall, J.A. *et al.* Essential role for retinoic acid in the promotion of CD4⁺ T cell effector responses via retinoic acid receptor α . *Immunity* **34**, 435–447 (2011).
19. Uematsu, S. *et al.* Regulation of humoral and cellular gut immunity by lamina propria dendritic cells expressing Toll-like receptor 5. *Nat. Immunol.* **9**, 769–776 (2008).
20. DePaolo, R.W. *et al.* Co-adjuvant effects of retinoic acid and IL-15 induce inflammatory immunity to dietary antigens. *Nature* **471**, 220–224 (2011).
21. Villablanca, E.J. *et al.* MyD88 and retinoic acid signaling pathways interact to modulate gastrointestinal activities of dendritic cells. *Gastroenterology* **141**, 176–185 (2011).
22. Chang, S.Y. *et al.* Lack of retinoic acid leads to increased langerin-expressing dendritic cells in gut-associated lymphoid tissues. *Gastroenterology* **138**, 1468–1478. 1478 e1461–1466 (2010).
23. Huber, S., Gagliani, N. & Flavell, R.A. Life, death, and miracles: Th17 cells in the intestine. *Eur. J. Immunol.* **42**, 2238–2245 (2012).
24. Zhu, Z. *et al.* Pulmonary expression of interleukin-13 causes inflammation, mucus hypersecretion, subepithelial fibrosis, physiologic abnormalities, and eotaxin production. *J. Clin. Invest.* **103**, 779–788 (1999).
25. Wynn, T.A. IL-13 effector functions. *Annu. Rev. Immunol.* **21**, 425–456 (2003).
26. Willis-Karp, M. Interleukin-13 in asthma pathogenesis. *Immunol. Rev.* **202**, 175–190 (2004).
27. Munitz, A., Brandt, E.B., Mingler, M., Finkelman, F.D. & Rothenberg, M.E. Distinct roles for IL-13 and IL-4 via IL-13 receptor $\alpha 1$ and the type II IL-4 receptor in asthma pathogenesis. *Proc. Natl. Acad. Sci. USA* **105**, 7240–7245 (2008).
28. Fuss, I.J. & Strober, W. The role of IL-13 and NK T cells in experimental and human ulcerative colitis. *Mucosal Immunol.* **1** (Suppl 1), S31–S33 (2008).
29. Hoving, J.C. *et al.* B cells that produce immunoglobulin E mediate colitis in BALB/c mice. *Gastroenterology* **142**, 96–108 (2012).
30. Akdis, M., Akdis, C.A., Weigl, L., Disch, R. & Blaser, K. Skin-homing, CLA⁺ memory T cells are activated in atopic dermatitis and regulate IgE by an IL-13-dominated cytokine pattern: IgG4 counter-regulation by CLA⁺ memory T cells. *J. Immunol.* **159**, 4611–4619 (1997).
31. Mora, J.R., Cheng, G., Picarella, D., Briskin, M., Buchanan, N. & von Andrian, U.H. Reciprocal and dynamic control of CD8 T cell homing by dendritic cells from skin- and gut-associated lymphoid tissues. *J. Exp. Med.* **201**, 303–316 (2005).
32. Ito, T. *et al.* TSLP-activated dendritic cells induce an inflammatory T helper type 2 cell response through OX40 ligand. *J. Exp. Med.* **202**, 1213–1223 (2005).
33. Hadeiba, H., Sato, T., Habtezion, A., Oderup, C., Pan, J. & Butcher, E.C. CCR9 expression defines tolerogenic plasmacytoid dendritic cells able to suppress acute graft-versus-host disease. *Nat. Immunol.* **9**, 1253–1260 (2008).
34. Besnard, A.G., Togbe, D., Guillou, N., Erard, F., Quesniaux, V. & Ryffel, B. IL-33-activated dendritic cells are critical for allergic airway inflammation. *Eur. J. Immunol.* **41**, 1675–1686 (2011).
35. Nakae, S. *et al.* Mast cells enhance T cell activation: importance of mast cell costimulatory molecules and secreted TNF. *J. Immunol.* **176**, 2238–2248 (2006).
36. McKenzie, G.J. *et al.* Impaired development of Th2 cells in IL-13-deficient mice. *Immunity* **9**, 423–432 (1998).
37. Mitsdoerffer, M. Proinflammatory T helper type 17 cells are effective B-cell helpers. *Proc. Natl. Acad. Sci. USA* **107**, 14292–14297 (2010).
38. Hino, A., Kweon, M.N., Fujihashi, K., McGhee, J.R. & Kiyono, H. Pathological role of large intestinal IL-12p40 for the induction of Th2-type allergic diarrhea. *Am. J. Pathol.* **164**, 1327–1335 (2004).
39. Hu, X. & Ivashkiv, L.B. Cross-regulation of signaling pathways by interferon-gamma: implications for immune responses and autoimmune diseases. *Immunity* **31**, 539–550 (2009).
40. Chang, J.H., Cha, H.R., Chang, S.Y., Ko, H.J., Seo, S.U. & Kweon, M.N. IFN- γ secreted by CD103⁺ dendritic cells leads to IgG generation in the mesenteric lymph node in the absence of vitamin A. *J. Immunol.* **186**, 6999–7005 (2011).
41. Newcomb, D.C. *et al.* A functional IL-13 receptor is expressed on polarized murine CD4⁺ Th17 cells and IL-13 signaling attenuates Th17 cytokine production. *J. Immunol.* **182**, 5317–5321 (2009).
42. Lajoie, S. *et al.* Complement-mediated regulation of the IL-17A axis is a central genetic determinant of the severity of experimental allergic asthma. *Nat. Immunol.* **11**, 928–935 (2010).
43. Ahmed, F., Jones, D.B. & Jackson, A.A. The interaction of vitamin A deficiency and rotavirus infection in the mouse. *Br. J. Nutr.* **63**, 363–373 (1990).
44. Gudas, L.J. Emerging roles for retinoids in regeneration and differentiation in normal and disease states. *Biochim. Biophys. Acta* **1821**, 213–221 (2012).
45. Mihaly, J., Gamlieli, A., Worm, M. & Ruhl, R. Decreased retinoid concentration and retinoid signalling pathways in human atopic dermatitis. *Exp. Dermatol.* **20**, 326–330 (2011).
46. Collins, C.B. *et al.* Retinoic acid attenuates ileitis by restoring the balance between T-helper 17 and T regulatory cells. *Gastroenterology* **141**, 1821–1831 (2011).
47. Mikhak, Z., Strassner, J.P. & Luster, A.D. Lung dendritic cells imprint T cell lung homing and promote lung immunity through the chemokine receptor CCR4. *J. Exp. Med.* **210**, 1855–1869 (2013).
48. Schuster, G.U., Kenyon, N.J. & Stephensen, C.B. Vitamin A deficiency decreases and high dietary vitamin A increases disease severity in the mouse model of asthma. *J. Immunol.* **180**, 1834–1842 (2008).
49. Allen, S., Britton, J.R. & Leonardi-Bee, J.A. Association between antioxidant vitamins and asthma outcome measures: systematic review and meta-analysis. *Thorax* **64**, 610–619 (2009).
50. Kang, S.G., Wang, C., Matsumoto, S. & Kim, C.H. High and low vitamin A therapies induce distinct FoxP3⁺ T-cell subsets and effectively control intestinal inflammation. *Gastroenterology* **137**, 1391–1402 e1391–1396 (2009).
51. Iliev, I.D. *et al.* Human intestinal epithelial cells promote the differentiation of tolerogenic dendritic cells. *Gut* **58**, 1481–1489 (2009).
52. Brown, C. *et al.* High prevalence of food sensitisation in young children with liver disease: a clue to food allergy pathogenesis? *Pediatr. Allergy Immunol.* **23**, 771–778 (2012).
53. Pino-Lagos, K. *et al.* A retinoic acid-dependent checkpoint in the development of CD4⁺ T cell-mediated immunity. *J. Exp. Med.* **208**, 1767–1775 (2011).
54. Ohoka, Y., Yokota, A., Takeuchi, H., Maeda, N. & Iwata, M. Retinoic acid-induced CCR9 expression requires transient TCR stimulation and cooperativity between NFATc2 and the retinoic acid receptor/retinoid X receptor complex. *J. Immunol.* **186**, 733–744 (2011).
55. Takeuchi, H. *et al.* Efficient induction of CCR9 on T cells requires coactivation of retinoic acid receptors and retinoid X receptors (RXRs): exaggerated T Cell homing to the intestine by RXR activation with organotins. *J. Immunol.* **185**, 5289–5299 (2010).

Original Article

Feasibility Re-evaluation of 75 mg/m² Docetaxel in Japanese Patients with Previously Treated Non-small Cell Lung Cancer

Kazuhiko Yamada*, Hiroaki Takeoka, Yusuke Mizoguchi, Fumie Yamashita, Tsukasa Yoshida, Yoshiaki Zaizen, Yusuke Okayama, Yoshiko Naito, Koichi Azuma and Tomoaki Hoshino

Division of Respiriology, Neurology, and Rheumatology, Department of Internal Medicine, Kurume University School of Medicine, Kurume City, Japan

*For reprints and all correspondence: Kazuhiko Yamada, Division of Respiriology, Neurology, and Rheumatology, Department of Internal Medicine, Kurume University School of Medicine, 67 Asahi-machi, Kurume City, Fukuoka 830-0011, Japan. E-mail: kayamada@med.kurume-u.ac.jp

Received September 13, 2013; accepted December 26, 2013

Objective: The primary objective of this study was to re-evaluate the feasibility of docetaxel at doses of up to 75 mg/m² in Japanese patients with previously treated non-small cell lung cancer.

Methods: Patients received escalated doses of docetaxel at 70 mg/m² (level 1) or 75 mg/m² (level 2) every 3 weeks until disease progression or unacceptable toxicities. Dose escalation was decided on the basis of dose-limiting toxicity in the first cycle of chemotherapy.

Results: At dose level 1, dose-limiting toxicity—Grade 3 febrile neutropenia—was observed in one of the six patients and at dose level 2, it was seen in one of the first six patients. Therefore, an additional 14 patients were enrolled at dose level 2, as originally planned. Among the total of 20 patients at dose level 2, 6 (<33%) developed dose-limiting toxicity in the first cycle: febrile neutropenia in 5 and pneumonia in 1. Finally, 10 (50%) of the 20 patients experienced toxicities that met the dose-limiting toxicity criteria, including 8 with febrile neutropenia throughout the treatment period, but this was manageable with dose reduction or appropriate supportive care. Other observed toxicities were predictable from the safety profile of docetaxel and were also well managed. Four partial responses were observed, giving an overall response rate of 15.4%. The median progression-free survival period of the patients overall was 4.0 months (95% confidence interval 1.4–6.6 months).

Conclusions: Although docetaxel administration at an initial dose of 75 mg/m² requires careful attention because of the high incidence of febrile neutropenia, this dose is considered feasible according to the protocol definition in Japanese patients with previously treated non-small cell lung cancer.

Key words: docetaxel – re-evaluation – Japanese – non-small cell lung cancer

INTRODUCTION

Currently in Japan, several agents (ex. docetaxel, pemetrexed, gefitinib, erlotinib or crizotinib) are recommended for use in patients with advanced or recurrent NSCLC that has progressed after platinum-based first-line chemotherapy based on the results of the clinical trials (1–6). Among these agents,

gefitinib and erlotinib are epidermal growth factor receptor tyrosine kinase inhibitors (EGFR-TKIs) and so they are used mainly for patients who have EGFR mutations (7–9). Because crizotinib is also a receptor tyrosine kinase inhibitor of anaplastic lymphoma kinase (ALK), it is only used for patients who have ALK rearrangements (10). With regard to pemetrexed, it has recently become clear that some specific

populations can benefit from the agent, for example those with non-squamous histology or low expression of thymidine synthase (11,12). Furthermore, pemetrexed has recently been used for both first-line chemotherapy and maintenance therapy (13). Therefore, the EGFR-TKIs, crizotinib and pemetrexed are used for limited populations of patients who can receive second- or third-line chemotherapies.

In contrast to such agents, docetaxel shows active cytotoxicity against various histological types of NSCLC by inhibiting microtubule depolymerization and promoting tubulin assembly in the M phase of the cell cycle, causing the cells to cease dividing. Docetaxel is usually administered at a dose of 75 mg/m² every 3 weeks in Western countries and almost in all Asian countries based on the results of two randomized controlled trials and a randomized phase II trial (1,2,14). In Japan, on the other hand, docetaxel has been administered at a relatively lower dose of 60 mg/m² in both clinical trials and clinical practice based on the recommended dose determined in a domestic phase I trial. However, the Japanese and Western studies demonstrated no significant difference in the pharmacokinetics (PK) of docetaxel (15).

Docetaxel is one of the most important cytotoxic agents for the treatment of NSCLC and is used as the reference regimen in clinical trials for previously treated NSCLC. Therefore, the difference in the recommended dose between Western and Japanese patients is a major problem for Japan when participating in global trials. The reason for the discrepancy in the maximum tolerated and recommended doses in comparison with Western studies remains unknown. Furthermore, no previously reported study has re-evaluated the safety, feasibility and efficacy of docetaxel at a dose of 75 mg/m², which is the global standard, since the drug was approved in Japan in 1997 (15). Therefore, we conducted the present study to reassess the safety, feasibility and efficacy of docetaxel at doses of up to 75 mg/m² in Japanese patients with previously treated NSCLC.

PATIENTS AND METHODS

STUDY DESIGN

The primary objective of this study was to re-evaluate the feasibility of docetaxel at doses of up to 75 mg/m² for Japanese patients with previously treated NSCLC.

Patients were divided into two docetaxel dose levels. At dose level 1, 6 patients received a dose of 70 mg/m². If three of these six patients experienced dose-limiting toxicity (DLT), dose escalation was terminated. If two of the patients or fewer experienced DLT, dose escalation was continued to the next level. At dose level 2, initially, the first six patients received docetaxel at 75 mg/m². If three of them experienced DLT, the study was terminated. If DLT was observed in 2 of the first 6 patients or fewer, additional patients, up to a maximum of 20, were enrolled to receive docetaxel at 75 mg/m². Dose escalation was decided according to whether DLT occurred only in the first cycle of chemotherapy, although toxicities

observed after the second cycle were taken into consideration in the final feasibility assessment.

PATIENT SELECTION

Patients with histologically or cytologically documented advanced or recurrent NSCLC, who had previously undergone platinum-based chemotherapy not including docetaxel-containing regimens, were eligible for study entry. An interval of at least 4 weeks from previous chemotherapy was required. Radiation therapy to a target lesion was allowed unless there was obvious disease progression in that lesion. Each patient was required to meet the following criteria: having measurable lesions; Eastern Cooperative Oncology Group (ECOG) performance status (PS) 0 or 1; age 75 years or less; SpO₂ ≥ 94%; normal 12-lead ECG; adequate bone marrow reserve [white blood cell (WBC) count ≥ 4000/μl, absolute neutrophil count (ANC) ≥ 2000/μl, platelet count ≥ 100 000/μl and hemoglobin ≥ 9.0 mg/dl]; and adequate hepatic and renal function (creatinine ≤ 1.5 mg/dl, total bilirubin ≤ 1.5 mg/dl and aspartate aminotransferase (AST) and alanine aminotransferase (ALT) levels ≤ 2.5 times upper limit of normal).

The main exclusion criteria were active concomitant malignancy, congestive heart failure, uncontrolled angina pectoris, arrhythmia, hypertension, uncontrolled diabetes, symptomatic infectious disease, severe hemorrhage/bleeding, pulmonary fibrosis or interstitial pneumonia, obstructive bowel disease or severe diarrhea, symptomatic peripheral effusion, cardiac effusion and ascites, ≥ Grade 2 peripheral neuropathy, symptomatic brain metastasis and pregnancy or breast feeding.

The study complied with the Declaration of Helsinki and Good Clinical Practice guidelines. The study protocol was approved by the institutional review board at Kurume University. All patients gave written informed consent prior to registration.

This study was registered with UMIN (University Hospital Medical Information Network in Japan), number UMIN 000003021.

STUDY TREATMENT

All patients received intravenous infusion of docetaxel over at least 60 min (70 or 75 mg/m²) every 3 weeks. Treatment was to be performed until disease progression, unacceptable toxicity or until the patients or the investigator requested treatment discontinuation. Subsequent cycles of treatment were withheld until the following criteria were satisfied: ECOG PS ≤ 1, ANC ≥ 2000/μl, platelet count ≥ 100 000/μl, total bilirubin ≤ 1.5 mg/dl, AST and ALT levels ≤ 2.5 times upper limit of normal, creatinine ≤ 1.5 mg/dl, SpO₂ ≥ 94%, absence of active infection and other non-hematological toxicity ≤ Grade 2. If these criteria were unsatisfied within 35 days from Day 1 of the current cycle, the patient was removed from the study. The docetaxel dose was reduced from 75 to 70 mg/m² (or 70–60 or 60–50 mg/m²) in the subsequent cycle if toxicity equivalent to DLT occurred. Prophylactic administration

of granulocyte colony-stimulating factor (G-CSF) was not allowed at any time during the study.

All patients underwent comprehensive baseline assessments including clinical laboratory tests and imaging studies. During the first cycle, clinical laboratory tests were performed at least twice a week. Patients also received follow-up assessments and monitoring at regular intervals thereafter. Toxicity evaluations were based on the Common Terminology Criteria for Adverse Events, version 3.0 (CTCAE v3.0) (16).

DEFINITION OF DLT

DLTs were defined as a toxicity occurring in Cycle 1 that met one of the following criteria and for which a causal relationship with docetaxel could not be ruled out: Grade 4 neutropenia lasting 7 days or longer, febrile neutropenia (FN), Grade 4 thrombocytopenia, Grade 3 thrombocytopenia that required platelet transfusion or was associated with bleeding, Grade 3 or 4 non-hematological toxicity (following events were to be DLT if the event did not recover to \leq Grade 2 despite standard/optimal supportive treatment: nausea, vomiting, anorexia, fatigue, constipation, diarrhea or transient electrolyte abnormality). If the patients experienced toxicities that met the DLT criteria, treatment doses were modified in subsequent courses.

SAFETY AND EFFICACY EVALUATION

All patients who received at least one dose of the study treatment were included in the safety and efficacy analysis. The incidence of adverse events was calculated for each dose group. The percentage decrease in ANC was also calculated from the baseline and nadir ANC. The efficacy endpoints were tumor response, progression-free survival (PFS) and overall survival (OS). Tumor response was evaluated according to the RECIST guideline and the distribution of the best overall responses was summarized in patients with target lesions (17). PFS was defined as the time from enrollment to the date of confirmation of progressive disease (PD) or the date of death from any cause, whichever was earlier. OS was defined as the time from registration until death from any cause. Patients not known to have died and to have had progression were censored at the date of the last progression-free assessment. Kaplan–Meier (K–M) methods were used for PFS and OS analyses. This included generating the K–M curve and determining the median with the 95% confidence interval. The survival data were cut off on 31 January 2013.

RESULTS

PATIENT CHARACTERISTICS

Between January 2010 and July 2012, 26 patients were enrolled into this study. Table 1 shows the characteristics of these patients. Twenty-three patients were male and three were female. The median age of the participants overall was 66 years (range 35–74 years). The majority of the patients had

Table 1. Patient characteristics

Characteristics	Level 1 (70 mg/m ²)	Level 2 (75 mg/m ²)
Number of patients	6	20
Gender		
Male/female	4/2	19/1
Age: median, years (range)	65 (62–70)	66 (35–74)
Performance status		
0/1	6/0	17/3
Histology		
Ad/Sq/Ad-Sq	3/2/1	16/4/0
Stage		
IIIA/IIIB	1/0	3/2
IV/relapse after surgery	4/1	12/3
EGFR mutation status		
Exon 19/exon 21	1/0	3/3
Wild type/unknown	3/2	9/5
Prior chemotherapy		
1/2	6/0	17/3
Paclitaxel containing	6	9

Ad, adenocarcinoma; Sq, squamous cell carcinoma; Ad-Sq, adenosquamous cell carcinoma; EGFR, epidermal growth factor receptor.

a PS of 0. Histologically, there were 19 adenocarcinomas and 6 squamous cell carcinomas. All but three patients received docetaxel as the second-line treatment. Seven of the 19 adenocarcinomas harbored EGFR mutations.

DOSE ESCALATION

The profiles of major toxicities and DLTs observed in Cycle 1 are shown in Table 2. At dose level 1, a DLT was observed in only one of six patients: Grade 3 FN. Apart from this DLT case, three patients at this dose level developed Grade 4 neutropenia, but the neutrophil count in these patients recovered rapidly without the use of G-CSF. Non-hematological toxicities were generally mild. The dose of docetaxel was then escalated to 75 mg/m² (level 2). At dose level 2, only one of the first six patients developed DLT: Grade 3 FN. Although all of the first six patients as well as this DLT case also developed Grade 3 or 4 neutropenia, the neutrophil count in these patients recovered rapidly without the use of G-CSF, similarly to level 1. Non-hematological toxicities were also generally mild. Therefore, an additional 14 patients were assigned to this dose level. In total, 20 patients were administered docetaxel at 75 mg/m².

TOXICITIES

The profiles of major toxicities and severe toxicities observed during the entire treatment period are shown in Tables 3 and 4. The hematological toxicities reaching \geq Grade 3 were

Table 2. Profile of major toxicities during the DLT period (Cycle 1)

Toxicities	Level 1 (n = 6)				Level 2 (n = 20)				Total (n = 26)
	Toxicity grade				Toxicity grade				Toxicity grade
	G1	G2	G3	G4	G1	G2	G3	G4	≤G2/≥G3 (G4)
Hematological									
Leukopenia	0	2	3	1	3	4	9	4	9/17 (5)
Neutropenia	0	1	0	5	0	4	3	13	5/21 (18)
Thrombocytopenia	3	0	0	0	3	0	0	0	6/0
Anemia	3	2	0	0	11	4	0	0	20/0
Non-hematological									
FN	—	—	1	0	—	—	5	0	—/6
Fatigue	4	0	0	0	7	0	0	0	11/0
Anorexia	2	0	0	0	4	2	0	0	8/0
Nausea	0	0	0	0	2	2	0	0	4/0
Stomatitis	0	0	0	0	2	0	0	0	2/0
Rash	1	0	0	0	4	0	0	0	5/0
Increased AST	1	0	0	0	2	0	0	0	3/0
Increased ALT	1	0	0	0	1	0	0	0	2/0
Increased GGT	2	1	0	0	2	0	0	0	5/0
Increased creatinine	2	0	0	0	3	0	0	0	5/0

DLT, dose-limiting toxicity; AST, aspartate aminotransferase; ALT, alanine aminotransferase; GGT, gamma-glutamyltransferase.

Table 3. Profile of major toxicities during the entire treatment period (all cycles)

Toxicities	Level 1 (n = 6)				Level 2 (n = 20)				Total (n = 26)
	Toxicity grade				Toxicity grade				Toxicity grade
	G1	G2	G3	G4	G1	G2	G3	G4	≤G2/≥G3 (G4)
Hematological									
Leukopenia	0	2	3	1	3	3	10	4	8/18 (5)
Neutropenia	0	0	1	5	0	3	4	13	3/23 (18)
Thrombocytopenia	3	0	0	0	2	0	0	1	5/1 (1)
Anemia	2	3	1	0	9	6	1	1	20/3 (1)
Non-hematological									
FN	—	—	2	0	—	—	8	0	—/10
Fatigue	6	0	0	0	8	3	0	0	17/0
Anorexia	3	0	0	0	7	4	0	0	13/0
Nausea	0	0	0	0	1	3	0	0	4/0
Stomatitis	1	0	0	0	3	2	0	0	6/0
Rash	1	0	0	0	5	0	0	0	6/0
Increased AST	1	0	0	0	3	0	1	0	4/1
Increased ALT	1	0	0	0	2	0	1	0	3/1
Increased GGT	2	1	0	0	4	0	0	0	7/0
Increased creatinine	2	0	0	0	2	0	1	0	4/1

Table 4. Individual patient data pertaining to toxicities that required dose reduction and treatment discontinuation

Patient	DLT	Toxicity equivalent to DLT after cycle 2	No. of treatment cycles	Dose reduction	Reason for discontinuation
Level 1					
1-1			2	No	PD
1-2		FN (cycle 4)	5	Yes	Delay (neutropenia)
1-3	FN		4	Yes	Refusal (fatigue)
1-4			2	No	PD
1-5			2	No	PD
1-6			22	No	PD
Level 2					
2-1			2	No	PD
2-2			6	No	PD
2-3		FN (cycle 5)	6	Yes	PD
2-4			8	No	Investigator's decision (edema limbs)
2-5			8	No	Delay (PS 2)
2-6	FN		7	Yes	Refusal (fatigue)
2-7	FN	Gastric hemorrhage (cycle 2), ILD (cycle 4)	4	Yes	TRD
2-8	Pneumonia		2	Yes	PD
2-9		FN (cycle 2)	6	Yes	PD
2-10			2	No	PD
2-11		Fatigue and anorexia (cycle 4)	5	Yes	PD
2-12	FN		4	Yes	PD
2-13			2	No	PD
2-14		ILD (cycle 2)	2	No	ILD
2-15			4	No	Investigator's decision (subungual abscess)
2-16		FN (cycle 3)	5	Yes	Refusal (fatigue)
2-17	FN		2	Yes	PD
2-18			3	No	PD
2-19			4	No	PD
2-20	FN		12	Yes	PD

PD, progressive disease; FN, febrile neutropenia; PS, performance status; ILD, interstitial lung disease; TRD, treatment-related death.

leukopenia (69%), neutropenia (88%), thrombocytopenia (4%) and anemia (12%). Of these, Grade 4 leukopenia and neutropenia were observed in 5 (19%) and 18 (69%) patients, respectively, but no patients required G-CSF except for those with FN, and all recovered promptly. The median duration of Grade 4 neutropenia was 4 days (range, 2–6 days). The mean percentage decrease in ANC was 87.5% (range, 50.2–98.7%) and there was no significant difference between dose levels 1 and 2 (87.9 and 87.4%, respectively, $P = 0.937$, unpaired t test). In addition, there was no significant correlation between the percentage decrease in ANC and age ($r = 0.199$, $P = 0.331$, Pearson's correlation coefficient). Red blood cell transfusion was performed in two patients, but no patients required platelet transfusion. With regard to non-hematological toxicity, 1 of 6 patients (17%) at dose level 1 and 5 of 20 patients (25%) at dose level 2 developed FN in the first cycle

(DLT period). For the 26 patients overall, there was no significant difference in age between those who developed FN and those who did not (mean, 62 versus 63 years, $P = 0.767$, unpaired t test). There was also no significant relationship between Grade 4 neutropenia (ANC < 500) and FN ($P = 0.132$, Fisher's exact test), although an ANC nadir of <200 resulted in an ~37-fold increase in the odds of FN (95% confidence interval (CI) 1.76–763, $P = 0.002$, Fisher's exact test). Although more than half of the patients experienced fatigue and anorexia, these were mostly transient and improved rapidly with standard/optimal supportive treatment. Other observed toxicities were predictable from the safety profile of decetaxel, and were well managed.

There was one treatment-related death in a 68-year-old man with adenocarcinoma that had progressed after initial chemoradiotherapy. He developed FN in the first cycle and gastric